CHAPTER 6

The Ozone Layer in the 21st Century

Lead Authors:
G.E. Bodeker
D.W. Waugh

Coauthors:
H. Akiyoshi
P. Braesicke
V. Eyring
D.W. Fahey
E. Manzini
M.J. Newchurch
R.W. Portmann
A. Robock
K.P. Shine
W. Steinbrecht
E.C. Weatherhead

Contributors:
J. Austin
S. Bekki
C. Brühl
N. Butchart
M. Chipperfield
M. Dameris
T. Egorova
V. Fioletov
A. Gettelman
M.A. Giorgetta
D. Kinnison
E. Mancini
M. Marchand
P.A. Newman
S. Pawson
G. Pitari
D. Plummer
B. Rognerud
E. Rozanov
R.J. Salawitch
T.G. Shepherd
K. Shibata
M. Sinnhuber
B.-M. Sinnhuber
S. Smyshlyaev
R. Stolarski
H. Struthers
W. Tian
G. Velders
D. Weisenstein
E.-S. Yang

CHAPTER 6

THE OZONE LAYER IN THE 21ST CENTURY

Contents

SCIENTIFIC SUMMARY

Global ozone levels are now no longer declining as they were from the late 1970s until the mid-1990s, and some increases in ozone have been observed. These improvements in the ozone layer have occurred during a period when stratospheric halogen abundances reached their peak and started to decline. These declining halogen abundances clearly reflect the success of the Montreal Protocol and its Amendments and Adjustments in controlling the global production and consumption of ozone-depleting substances (ODSs).

Stratospheric ozone abundances are affected by a number of natural and anthropogenic factors in addition to the atmospheric abundance of ODSs, e.g., temperatures, transport, volcanoes, solar activity, and hydrogen and nitrogen oxides (Chapter 3). Separating the effects of these factors is complex because of nonlinearities and feedbacks in the atmospheric processes affecting ozone. For the purposes of this Assessment, we consider specifically the recovery of ozone from the effects of ODSs, because the primary audience is the group of Parties to the Montreal Protocol, whose purview is ozone-depleting compounds. In this Assessment, the metric used to gauge the overall burden of ozone-depleting halogens in the stratosphere from the ODSs is equivalent effective stratospheric chlorine (EESC).

The Process of Ozone Recovery from the Effects of ODSs

- In this Assessment, the recovery of ozone from depletion caused by increases in ODSs is discussed as a process involving three stages:

  (i) The **slowing of ozone decline,** identified as the occurrence of a statistically significant reduction in the rate of decline in ozone due to changing EESC.

  (ii) The **onset of ozone increases (turnaround),** identified as the occurrence of statistically significant increases in ozone above previous minimum values due to declining EESC.

  (iii) The **full recovery of ozone from ODSs,** identified as when ozone is no longer significantly affected by ODSs. In the absence of changes in the sensitivity of ozone to ODSs, this is likely to occur when EESC returns to pre-1980 levels.

  The first two stages of recovery either have already occurred or are expected to occur within the next two decades. The third stage is expected to occur around the middle of the century. Because of changes in atmospheric composition and dynamics, this third stage may or may not be accompanied by the actual return of ozone to pre-1980 levels, and it is possible that ozone could return to 1980 levels before the effects of ODSs disappear.

- In reaching full recovery of ozone, the milestone of **the return of ozone to pre-1980 levels** is considered important because ozone was not significantly affected by ODSs prior to 1980. As a consequence, this milestone is useful, for example, to gauge when the adverse impacts of enhanced surface ultraviolet (UV) radiation on human health and ecosystems caused by ozone depletion are likely to become negligible. However, as mentioned above, the return of ozone to pre-1980 levels may not occur at the same time as the return of EESC to pre-1980 levels, and in fact may never occur because of changes in the atmosphere since 1980 that are not caused by ODSs. Therefore, this milestone alone cannot be used to identify the recovery of ozone from the effects of ODSs.

The Role of ODSs in Recent Ozone Trends

- **The slowing of the decline and leveling off of midlatitude upper stratospheric (35-45 km) ozone over the past decade has very likely been dominated by changes in EESC.** Gas-phase chemistry, modulated by changes in temperature and other gases such as methane (CH_4), directly controls ozone in this region, and observed ozone changes are similar to those modeled from EESC decreases.

- **Over the past decade, changes in EESC have likely contributed to the slowing of the midlatitude total column ozone decline and the leveling off of ozone.** However, evidence suggests that changes in transport have also played an important role, particularly in the lowermost stratosphere, making attribution of specific ozone changes to EESC more complicated. For northern midlatitudes, increases in ozone have been greater than expected from

EESC decreases alone, while over southern midlatitudes the observed ozone changes are broadly consistent with the expectations from EESC decreases alone.

- **Inside the Antarctic vortex, the interannual variations in ozone depletion observed from 2001 to 2005 have not been caused by changes in EESC.** At current EESC concentrations, nearly total loss of ozone occurs in the lowermost stratosphere inside the ozone hole in September and October, and EESC concentrations often exceed those necessary to cause total loss. The Antarctic ozone hole, therefore, has low sensitivity to moderate decreases in EESC and the unusually small ozone holes in some recent years (e.g., 2002 and 2004) are strongly attributable to a dynamically driven warmer Antarctic stratosphere.

- **In the collar region of the Antarctic vortex (60°S-70°S), where ozone destruction is not complete, reductions in EESC have likely contributed to the slowing of ozone decline observed over the past decade.** However, uncertainty in the estimation of EESC in the collar region and the ozone response to temperature changes confound the attribution of observed ozone changes to reductions in EESC.

- **The decline in EESC has not caused the large interannual variations observed in Arctic ozone depletion.** Indeed there has been no detection of any ozone recovery stages in the Arctic. The large interannual variations in ozone are driven by changes in meteorology and are likely to delay the detection of the first stage of recovery.

Expected Future Changes in Ozone

Two-dimensional (2-D) models and three-dimensional (3-D) coupled Chemistry-Climate Models (CCMs), both of which have achieved significant successes in simulating many or nearly all of the factors that affect ozone and their feedbacks, have been used to project the evolution of ozone throughout the 21st century. The evolution of tropical and midlatitude ozone was examined in all models. CCMs are generally believed to better represent key processes relating to three-dimensional transport in the polar regions and, therefore, only CCMs were used for polar regions. The projected total column ozone was examined for three periods:

(i) The beginning of the century (2000-2020), when EESC is expected to start decreasing or continue to decrease

(ii) Mid-century (2040-2050 in extrapolar regions, 2060-2070 in polar regions), when EESC is expected to reach and fall below 1980 values

(iii) End of the century (2090-2100), when changes in factors other than ODSs are expected to control changes in stratospheric ozone

Because modeled changes in column ozone to 2100 are not specifically attributable to changes in EESC, ozone column amounts when EESC returns to pre-1980 levels and the timing of the return of ozone to pre-1980 levels are examined in the model projections.

- **The CCMs used to project future ozone abundances have been critically evaluated, and more emphasis has been given to those models that best represent the processes known to strongly affect column ozone abundances.** The CCMs vary in their skill in representing different processes and characteristics of the atmosphere. However, there is sufficient agreement between the majority of the CCMs and the observations that some confidence can be placed in their projections.

Beginning of the Century

- **Averaged between 60°S and 60°N, total column ozone is projected to increase in all models between 2000 and 2020, with most of the increase of 1 to 2.5% occurring after 2010.** The small interannual variability shown in 2-D models allows more precise identification of key ozone change dates compared with CCMs that show large interannual variability, similar to that seen in observations. Nonetheless, both the 2-D models and CCMs suggest that minimum total column ozone values have already occurred in this latitude region.

.• **Over the Antarctic, most CCMs predict column ozone increases in spring of around 5 to 10% between 2000 and 2020. Different diagnostics of ozone depletion show different sensitivities to EESC.** The most rapid change (decrease) occurs in the ozone mass deficit and the slowest change (increase) in ozone minimum values and October ozone anomalies. Minimum ozone values remain roughly constant between 2000 and 2010 in many models. The projected onset of decreases in the ozone mass deficit occurs between 2000 and 2005, whereas the projected onset of increases in minimum Antarctic ozone does not occur until after 2010 in many models.

• **Over the Arctic, most CCMs predict that springtime column ozone in 2020 will be 0 to 10% above 2000 levels and that ozone turnaround in the Arctic will occur before 2020.** Over the Arctic, the large interannual variability in the CCM projections obscures the year when the ozone turnaround due to decreasing EESC occurs.

Mid-Century

• **Averaged between 60°S and 60°N, total column ozone is projected to be close to or above 1980 values when EESC in that region of the stratosphere declines to 1980 values (2040-2050).** This occurs in nearly all models that include coupling between well-mixed greenhouse gases (WMGHGs; carbon dioxide (CO_2), methane (CH_4), and nitrous oxide (N_2O)) and temperature (interactive 2-D models and the CCMs). Thus, outside polar regions, ozone is projected to reach 1980 values at about the same time or before EESC returns to 1980 values.

• **Two-dimensional models that include coupling between WMGHGs and temperature (interactive 2-D models) predict that column ozone averaged over 60°S to 60°N will in general exceed 1980 values up to 15 years earlier than models that do not include these feedbacks (non-interactive 2-D models).** This suggests that the earlier return to 1980 values is caused mainly by response to stratospheric cooling linked to increased WMGHGs. The response results from the temperature dependence of the gas-phase photochemistry of ozone. In some non-interactive 2-D models, column ozone never increases to 1980 values throughout the 21st century in some regions.

• **Over the Antarctic, most models predict that ozone amounts will increase to 1980 values close to the time when Antarctic EESC decreases to 1980 values.** That time is later than at midlatitudes due to the delay associated with transport of stratospheric air to polar regions. A new empirical model, based on observations, indicates a return of Antarctic EESC to 1980 values between 2060 and 2075.

• **Over the Arctic, CCMs show ozone values exceeding 1980 values before EESC decreases to 1980 values, with ozone increasing to 1980 values between 2020 and 2040.** The increases in ozone do not follow the decreases in EESC as closely as in the Antarctic, and in the majority of CCMs Arctic ozone exceeds 1980 values before the Antarctic. There is no indication of future severe reductions in Arctic column ozone in any of the model simulations. There is large uncertainty in projections of Arctic ozone because of the smaller ozone depletion and the larger interannual variability in the Arctic stratosphere in comparison with the Antarctic.

End of the Century

• **Averaged between 60°S and 60°N, total column ozone is projected to be around 2 to 5% above 1980 values between 2090 and 2100.** This result is obtained in all 2-D models that include coupling between WMGHGs and temperature and in one CCM that extends to 2100. This CCM predicts that from 2090 to 2100, Arctic ozone will be substantially above 1980 values, while Antarctic ozone will be close to or just below 1980 values.

• **Projected ozone amounts in 2100 are sensitive to future levels of WMGHGs.** For example, expected future increases in N_2O will increase stratospheric nitrogen oxides (NO_x), which may exacerbate ozone depletion. However, the expected stratospheric cooling induced by increasing concentrations of greenhouse gases, primarily CO_2, is expected to slow gas-phase ozone depletion reactions and, thereby, increase ozone. The net effect on ozone amounts will depend on future levels of the different WMGHGs. The importance of this temperature feedback is demonstrated by the non-interactive 2-D models, which predict that extrapolar column ozone will be less than or near 1980 values through the latter half of the century.

6.1 INTRODUCTION

It is now clear that the depletion of the ozone layer, both globally and in the polar regions, is attributable to an atmospheric halogen burden that is strongly enhanced compared with natural levels by anthropogenic emissions of ozone-depleting substances (ODSs). Over the past decade, as a consequence of adherence to the Montreal Protocol and its Amendments and Adjustments, equivalent effective stratospheric chlorine (EESC; see Chapter 8), a commonly used measure of the stratospheric halogen burden, has peaked and begun to decline (Chapter 1). However, owing to the long lifetime of the most important halogen source gases, the removal of ODSs from the atmosphere will take many decades even with continued compliance with the Montreal Protocol (Chapter 8). Ozone is expected to continue to respond to these changes in ODSs but the timing and sensitivity of the response will depend on other changes in the atmosphere, e.g., increases in well-mixed greenhouse gases (WMGHGs) that have occurred since the onset of significant ozone depletion in 1980.

Chapters 3 and 4 discuss ozone changes observed to date and interpret the underlying causes of the changes, while Chapter 5 examines the mechanisms connecting ozone depletion with climate change. This chapter builds on the material presented in these three chapters, with a focus on two overarching themes:

(1) Analysis of recent ozone measurements for the first signs of ozone recovery attributable to decreasing ODS concentrations
(2) Projections of how the global ozone layer will evolve during the 21st century and how this evolution will depend on ODSs and other concomitant changes in the atmosphere

The first of these two themes uses the observational time series presented in Chapters 3 and 4 to assess whether ozone recovery (defined in Section 6.2) has been detected. The interpretation of observations presented in the two earlier chapters is extended by applying different statistical tools (Section 6.4) to the detection of the first stage of ozone recovery, i.e., a slowing of the ozone decline attributable to decreasing ODSs. This chapter also examines when increases in ozone due to decreases in ODSs are likely to occur, i.e., the second stage in the ozone recovery process.

The second theme builds on the discussion of the feedbacks between ozone depletion and climate change presented in Chapter 5. A group of two-dimensional (2-D) models and coupled Chemistry-Climate Models (CCMs), incorporating climate feedback processes, is used to predict the evolution of the ozone layer throughout the 21st century. While Chapter 5 discusses ozone depletion/climate change interactions, this chapter uses models to investigate the effects of those interactions and addresses how they may affect the evolution of ozone throughout this century. The resulting ozone projections are then used in Chapter 7 to show how surface clear-sky ultraviolet (UV) radiation is expected to change in the future.

Section 6.2 describes the framework for assessing ozone changes through the 21st century. Specifically it discusses the time scales of the expected changes, stages in the recovery process and the milestones defining those stages. Section 6.3 includes a discussion of how factors other than ODSs affect the detection and timing of milestones in the ozone recovery process and the attribution to changing EESC. Section 6.4 presents how least squares regression models (also discussed in Chapter 3) can be used to evaluate the role of ODSs and other factors in ozone recovery. The interpretation of recent observations of ozone in the context of ozone recovery is presented in Section 6.5. The longer-term perspective of the evolution of global ozone through the 21st century is provided in Section 6.6, where the results from the 2-D models and CCMs are assessed.

6.2 A FRAMEWORK FOR EVALUATING CHANGES IN OZONE ABUNDANCES

In considering the ozone layer in the 21st century, two topics are prominent in the scientific and policy communities. The first is obtaining evidence as soon as possible that the ozone layer is responding to the decline in EESC. As ODSs are removed from the atmosphere, the destruction of ozone attributed to ODSs is also expected to decline. The second topic is the projection of changes that might occur in the ozone layer by mid-century and by the end of the century. By approximately mid-century, substantial or full recovery of the ozone layer is expected globally. By the end of the century, other changes in atmospheric chemistry and transport become a prominent consideration in projected ozone amounts. Here, we have adopted a specific framework, described below, to evaluate changes in ozone over the recent past and until the end of the century. This framework is conceptual in design and is intended to encompass both ozone changes that have already occurred as well as potential future changes.

6.2.1 Ozone Changes in the Near and Long Term

The discussion of ozone changes in the 21st century is divided into those in the "near term," which includes the recent past, the present day, and the first decades of

the century, and those in the "long term," which includes the remaining decades of this century. In the near term, when ozone observations and model simulations can be compared, the first changes in the ozone layer attributable to the ongoing removal of ODSs can be detected. In contrast, changes in the last decades of this century can only be discussed as model projections and, hence, are associated with large uncertainties.

Within each time period, the analyses of ozone changes will focus separately on changes that occur, for example, in global average total column ozone, midlatitude and tropical column ozone, as well as springtime polar ozone amounts. The role of ODSs in ozone changes is of particular importance, but the role of other factors, such as changes in abundances of other gases and of sulfate aerosols, stratospheric temperatures, atmospheric transport, solar output, and volcanic emissions, will also be carefully examined (see Section 6.3). Without a comprehensive examination of all factors that significantly influence ozone amounts, the contribution of ODSs cannot be quantified with sufficient confidence.

6.2.2 Stages in the Evolution of the Ozone Layer

Ozone changes in the 21st century are expected to encompass the period of the "recovery" of ozone from the influence of ODSs that have been released in anthropogenic activities. ODSs have led to the decline in global ozone amounts, with measurable changes beginning in the 1980s and the largest changes found in the winter/spring polar stratospheres (see Chapters 3 and 4). The total abundance of ODSs is in decline in the troposphere and stratosphere as a result of the effective actions undertaken as part of the Montreal Protocol (see Chapter 1). The start of the decline in EESC marks the conceptual start of the ozone recovery process. The continued analysis of ozone measurements

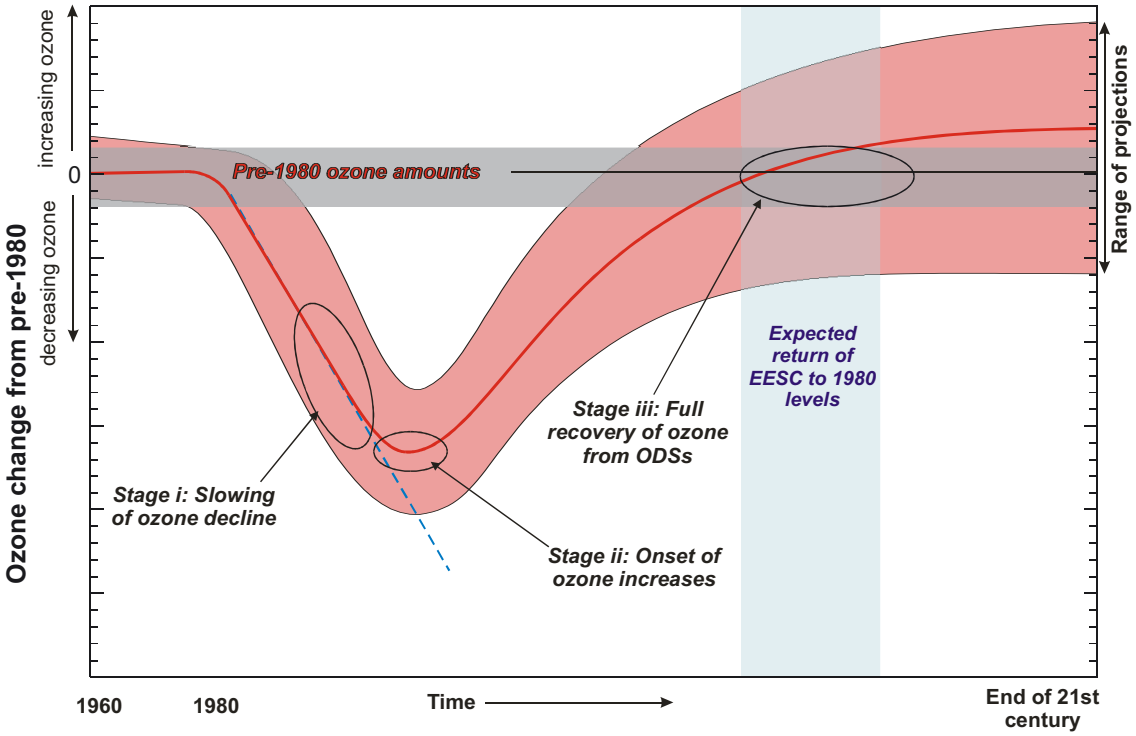

Figure 6-1. A schematic diagram of the temporal evolution of global ozone amounts beginning with pre-1980 values, which represent amounts before significant depletion due to anthropogenic ODS emissions, and stopping at the end of the 21st century. Observed and expected ozone amounts (solid red line) show depletion from pre-1980 values and the three stages of recovery from this depletion (see Section 6.2). The red-shaded region represents the range of observations and model results for both near-term and long-term ozone changes. The blue-shaded region represents the time period when declining global ODS concentrations are expected to reach 1980 values. The full recovery of ozone from ODSs may be delayed beyond the return of ODSs to 1980 levels by factors (e.g., a volcanic eruption close to that time) that could change the sensitivity of ozone to ODSs.

during the 21st century is expected to reveal and confirm three key stages in the recovery process:

(i) The **slowing of ozone decline**, identified as the occurrence of a statistically significant reduction in the rate of decline in ozone due to changing EESC
(ii) The **onset of ozone increases (turnaround)**, identified as the occurrence of statistically significant increases in ozone above previous minimum values due to declining EESC
(iii) The **full recovery of ozone from ODSs**, identified as when ozone is no longer affected by ODSs. In the absence of changes in the sensitivity of ozone to ODSs, this is likely to occur when EESC returns to pre-1980 levels

As illustrated in Figure 6-1, the first two stages of recovery are expected to occur in the near term and the last stage in the long-term future. These three stages apply to both total column ozone and ozone at a specific altitude. However, the timing of the stages may be different for these different measures of ozone. Documenting how and when each of these stages of ozone layer recovery is reached will be of interest to both the scientific and policy communities.

The focus of this chapter is how, and to what extent, observed and projected changes in ozone during the recovery process will be attributable to changes in ODSs and to other contributing factors as noted above.

The role of contributing factors in the recovery process is important because the physical and chemical environment of the atmosphere has changed significantly since the onset of observable ozone depletion in the 1980s. A key aspect of ozone recovery is whether or not ozone abundances in stage (iii) will be greater than or less than those present in 1980 before significant depletion by ODSs occurred. As shown in Figure 6-1, projections of ozone abundances show a range of values during the full recovery stage because of uncertainties in the role of contributing factors in controlling ozone in the coming decades. At present there is no standard definition of stages in the ozone recovery process and no standard framework that can be used to analyze ozone observations for signs of recovery. Authors of previous studies have used terms such as "recovery" with a range of different meanings. For example, not all studies have incorporated the concept of attribution in the definition of ozone recovery. The framework presented here with three defined stages of ozone recovery will provide a more rigorous basis for future analyses of ozone changes.

6.2.3 Milestones in the Evolution of the Ozone Layer

The stages of recovery outlined above apply to the overall response of the ozone layer. As an aid to monitoring and documenting each stage of recovery, *milestones* can be defined within the recovery stages. A milestone is a point in a recovery stage that a specific change in a specific ozone parameter can be said to have occurred. Milestones and milestone parameters reflect that ozone changes during the recovery process will vary with geographic region and altitude, following in large part the known variations and differences in ozone depletion. Primary geographic regions are the Antarctic and Arctic regions, midlatitudes, and the tropics. Primary altitude regions are the upper and lower stratosphere. Table 6-1 summarizes a number of possible milestone parameters, some of which will be discussed in the following sections.

Table 6-1. Examples of milestone parameters in ozone recovery stages.

Stratospheric Region	Milestone Parameters
Antarctic during winter/early spring (60°S-90°S)	Daily minimum column ozone values Minimum values of the ozone partial column between 12 and 20 km above the South Pole Area of the 220 DU contour of the ozone hole Vortex average daily ozone mass deficit Seasonal trend in average column ozone
Arctic during winter/early spring (60°N-90°N)	Daily minimum column ozone values Seasonal trend in average column ozone
Midlatitudes (35°-60°)	Trend in column ozone Trend in upper stratospheric column ozone (35-45 km) Trend in lower stratospheric ozone (15-20 km)
Tropics (25°N-25°S)	Trend in column ozone

Milestone parameters are all quantifiable from observational datasets. A milestone derives directly from a parameter by choosing a quantitative threshold or limit value. Reaching or passing a milestone then has a quantitative and statistical basis that can be objectively evaluated. For example, milestones derive easily from parameters associated with trends in Table 6-1:

Milestone 1: the year(s) when the negative ozone trends seen in the 1980s and 1990s begin to weaken (related to Stage (i))

Milestone 2: the year(s) that there is a trend reversal (related to Stage (ii))

Milestone 3: the year(s) that EESC returns to pre-1980 values

Milestone 4: the year(s) that the parameter reaches pre-1980 values (related to Stage (iii))

Clearly, many milestones can be defined using the parameters listed and the expectations of the stages of ozone recovery as outlined above and as temporally displayed in Figure 6-1. Of greatest interest and importance are those milestones that primarily result from changes in ODS amounts, that will occur soonest, and that will have the largest statistical significance using available observational datasets. Also of interest are those milestones that can be simulated in global models of ozone recovery using known changes in ODSs.

6.2.4 Using Data and Models to Evaluate Ozone Milestones and Milestone Parameters

The principal tools to evaluate ozone milestone parameters are statistical analyses of ozone observations, the results of global models for past ozone amounts, and the model projections of future amounts. Observational time series are available from multiple sources, including satellite-, ground-, aircraft-, and balloon-based instruments. Each has a role in documenting ozone parameters over time in profile and column amounts, and each has value in establishing accurate ozone trends. Statistical tools are required to derive ozone trends because ozone amounts are subject to significant natural variability throughout the available time series and the quality of ozone data is not uniform. The variability arises because ozone amounts reflect transport as well as chemical production and loss processes that are affected by a wide range of factors as noted in Sections 6.2.1 and 6.3, and Section 3.4 of Chapter 3.

Models and statistical methods are key tools in the attribution of changes in milestone parameters to the various controlling factors. Statistical analyses of time series are used to derive trends and their uncertainties (see Chapter 3). Photochemical box models constrained by observations of chemical composition are useful for quantifying the role of ODS changes in observed parameter changes. More complex models are needed to address global ozone changes caused by the full range of contributing factors; namely, changes in atmospheric composition, stratospheric temperatures, atmospheric transport, solar output, and volcanic emissions. Those relied upon in this Assessment are 2-D models and CCMs. Descriptions of these models are provided in Chapter 5 while the role of each model in this chapter is detailed in the following sections. An important challenge for these models is to represent the atmospheric processes sufficiently well that observed changes can be understood and attribution of changes can be discussed. A large source of uncertainty in model projections of ozone is the scenarios that must be adopted by the models to account for changes in atmospheric parameters related to climate change.

6.3 FACTORS AFFECTING THE DETECTION, ATTRIBUTION, AND TIMING OF MILESTONES

In this section we discuss to what extent different factors contributing to the variability in stratospheric ozone are likely to affect the detection, attribution, and timing of milestones. A major issue is the variability in ozone induced by these factors that masks or resembles the expected ozone change due to halogen loading (see Figure 3-1 of Chapter 3). For projections over the rest of the century, the issue is how factors other than ODSs may change the expected increases in ozone from decreasing halogen loading.

6.3.1 Stratospheric Halogen Loading

The evolution of stratospheric halogen loading is an obvious factor impacting ozone. Correctly estimating stratospheric halogen loading is important for attributing observed changes in ozone to decreases in EESC. The global mean EESC from WMO (2003) is generally used in such studies. However, if the estimated EESC is incorrect or not appropriate for the region being considered, then the attribution or inferred timing of a milestone may be incorrect. Possible causes of incorrect EESC include using an inappropriate mean age of air, neglecting mixing processes in the atmosphere (i.e., neglect of age spectra), or incorrectly accounting for the bromine contribution (see Chapter 1). The effect of errors in EESC estimation is most likely largest for the detection of milestones in polar regions, where the EESC from WMO (2003) peaks too

early and decays too rapidly because of the older mean age of air in polar regions and the neglect of the age spectra (see Newman et al., 2006, and the figure in Box 8-1 of Chapter 8).

Future stratospheric halogen concentrations will depend on future emissions of ODSs and on transport into and through the stratosphere. Model simulations suggest that increases in WMGHGs (carbon dioxide (CO_2), nitrous oxide (N_2O), and methane (CH_4)) may lead to an increased stratospheric circulation and to reduced transport time scales (e.g., Butchart and Scaife, 2001; Butchart et al., 2006; Section 5.3.3 of Chapter 5). A reduction in transport time scales will result in a reduction of EESC, which could affect the timing of long-term milestones.

6.3.2 Atmospheric Chemical Composition

Apart from changing ODSs, changes in other gases could affect the evolution of ozone and the timing of ozone recovery by changing the background chemical composition of the atmosphere. In particular, increases in gases producing radicals that catalytically destroy ozone (e.g., N_2O, CH_4, molecular hydrogen (H_2), and water (H_2O)) are likely to change ozone. As discussed in Section 6.3.3, temperature changes due to WMGHGs are also important. Section 1.4 of Chapter 1 discusses the possible long-term changes in gases other than ODSs that may affect ozone and Section 6.6 discusses model estimates of ozone evolution based on emission scenarios of these gases.

Catalytic ozone loss in the stratosphere occurs from the reactive nitrogen (NO_x), hydrogen (HO_x), oxygen (O_x), chlorine (ClO_x), and bromine (BrO_x) families. Ozone loss through these families is strongly altitude and latitude dependent (see Figure 1.11 of IPCC/TEAP, 2005), with NO_x dominating in the middle stratosphere (approximately 25-40 km), and HO_x dominating in the lower and upper stratosphere. Under conditions of high chlorine loading, ClO_x is important in the upper stratosphere (peak impact near 40 km) and in regions where heterogeneous reaction rates are large, such as in the polar regions during spring. However, in many regions of the stratosphere, these changes are strongly buffered by induced changes on the other chemical families, which can reduce the primary impact (Nevison et al., 1999). For example, NO_x increases in the lower stratosphere cause decreases in HO_x and ClO_x catalyzed losses, along with increases in "tropospheric" ozone production mechanisms. In the middle stratosphere, NO_x induced changes are reduced by interactions with chlorine species. On the other hand, in some cases coupling between different chemical processes can amplify the effects of source gas emissions, e.g., nitrogen dioxide (NO_2) concentrations over southern midlatitudes have risen at approximately twice the rate of its source gas N_2O as a result of changes in ozone (Section 3.3.2 of Chapter 3; McLinden et al., 2001).

Another compositional change that could affect ozone is a change in stratospheric water vapor. An increase in water vapor would increase HO_x and thus cause ozone decreases in the upper and lower stratosphere (Kirk-Davidoff et al., 1999; Dvortsov and Solomon, 2001), although these changes are reduced by complex buffering interactions. In the polar regions, increases in water vapor would cause an increase in heterogeneous reaction rates (e.g., hydrogen chloride (HCl) plus chlorine nitrate ($ClONO_2$)) and an increase in the surface areas of polar stratospheric cloud (PSC) particles. Both effects are likely to lead to an increase in chlorine activation and ozone loss. The effects of water vapor increases on ozone (via HO_x), induced by increases in methane, are partially offset by the reaction of methane with atomic chlorine, which deactivates ClO_x and reduces ClO_x-driven ozone loss (this could be important throughout the stratosphere). The coupling of water vapor and methane with ClO_x induced ozone loss will be eliminated by decreasing ODS levels during the 21st century.

While the Assessment does not deal with tropospheric ozone per se, it should be noted that increases in tropospheric ozone in some regions might have masked stratospheric decreases (such as in the tropics, where stratospheric decreases are relatively small). In such regions, total column ozone measurements cannot be used for detection and attribution of recovery milestones, and vertical ozone profile data are required. Vertically resolved observations in the stratosphere allow separation of regions controlled by ODSs and those dominated by transport (see Section 6.5).

6.3.3 Stratospheric Temperatures

As discussed in Chapter 5, the rates of chemical reactions, and the formation of PSCs, depend on temperature. Thus, changes in temperature can have a large influence on ozone. Temperature changes need to be accounted for when attributing observed ozone variations to changes in halogen loading and when predicting future ozone levels. This is especially important for attribution in polar regions, where interannual variations in ozone are closely coupled to variations in polar temperatures; in the Arctic, ozone loss rates are related to the volume of PSCs (e.g., Rex et al., 2004), whereas in the Antarctic, the size of the ozone hole depends on the temperature in the vortex "collar region" (60°S-70°S) (e.g., Newman et al., 2004).

Future stratospheric temperatures are a major source of uncertainty when predicting future ozone levels.

They are a key parameter for the questions of whether and when ozone will return to pre-1980 levels. As discussed in Chapter 5, stratospheric temperatures depend on stratospheric dynamics, radiation, and composition. Future changes in temperature, and hence ozone, are not likely to be uniform throughout the stratosphere. Cooling due to increased CO_2 (and other WMGHGs), particularly in the upper stratosphere, is expected to slow gas-phase ozone loss reactions. When EESC decreases to pre-1980 levels, and if there are no other changes, the cooling will lead to an increase in ozone to values higher than in 1980. However, as noted in the previous subsection, increases in WMGHGs will also alter the chemical composition of the stratosphere and possibly the Brewer-Dobson circulation. These effects are also likely to affect ozone; see Section 6.6 for further discussion. The impact of stratospheric cooling on ozone might be the opposite in polar regions. Here, cooling could result in increases in PSCs, which, given enough halogens, would increase ozone loss.

6.3.4 Atmospheric Transport

Atmospheric transport is a major factor contributing to stratospheric ozone variability. Accounting for this variability is an important issue both for detecting and attributing ozone recovery milestones. As discussed in Chapters 3 and 4, changes in the stratospheric meridional circulation, in the stratospheric polar vortices, and in tropospheric weather systems, all have a strong influence on stratospheric ozone and can produce variability on a wide range of time scales. Some of these changes can be linked to waves propagating from the troposphere, but internal stratospheric dynamics also play a role.

The detection of recovery milestones is essentially a signal-to-noise ratio problem, and much of the "noise" in the ozone signal results from variability in transport. Geographical differences in the variability in ozone induced by this factor will affect where and when certain recovery milestones can best be detected. Alternatively, it determines the number of years of measurements required to detect a milestone. Reinsel et al. (2002) found that for midlatitudes (30°-60°), a statistically significant change in total column ozone trend can be detected with ~7-8 years of data following the period of linear decline, whereas detection of ozone turnaround (the second stage in the ozone recovery process) can require ~15-20 years for southern midlatitude zonal average column ozone and ~20-25 years for northern midlatitude zonal average column ozone. This result is in agreement with earlier findings (Weatherhead et al., 2000). Analyzing vertically resolved atmospheric regions is an effective technique to increase the signal-to-noise ratio because of the vertical separation of the forcing functions (Yang et al., 2006; Weatherhead and Andersen, 2006).

Statistical regression models are often used to remove competing drivers of ozone variability in the attribution of ozone changes to ODSs. They are based on the assumption that proxies describing the dynamical state of the atmosphere and resultant effects on ozone can be provided as model basis functions. Commonly used dynamical proxies are equatorial zonal winds to capture the effects of the quasi-biennial oscillation (QBO), the Arctic Oscillation or Antarctic Oscillation (AO or AAO), the North Atlantic Oscillation (NAO), the El Niño Southern Oscillation (ENSO) index, and measures of wave activity (e.g., latitudinally averaged tropopause Eliassen-Palm fluxes). However, because such preselected proxies are not necessarily independent (they are not orthogonal within the regression model), the partitioning of the ozone variance among the different proxies by the model requires some interpretation. It is difficult to establish how much of the transport-driven ozone variability is appropriately accounted for. An alternative approach is to use idealized modeling studies to quantify the impact of different circulation regimes on ozone. For example, the magnitude of ozone changes related to a strong warm ENSO event was investigated by Brönnimann et al. (2004) and Pyle et al. (2005).

Changes in temperatures and transport not only complicate the detection and attribution of recovery milestones, they also affect ozone projections over the rest of this century (see Chapter 5).

6.3.5 The Solar Cycle

When attributing recent changes in stratospheric ozone to changes in ODSs, it is important to consider ozone variations related to the 11-year solar cycle because the timing of the most recent maximum in solar activity, between 1999 and 2003, was around the time when EESC peaked in the stratosphere. As discussed in Chapter 3, observations continue to indicate a statistically significant solar variation of ozone, with ozone in phase with solar activity. This suggests that an increase in solar activity during the 1999-2003 solar maximum will have contributed to the slowing of the decline and increase of ozone (e.g., Dameris et al., 2006). Proper attribution of the cause of the ozone changes in recent years requires the separation of ozone increases due to changes in solar irradiance from those due to changes in halogen levels. However, this is difficult, as the magnitude of the solar influence on ozone is somewhat uncertain.

The amplitude of ozone changes due to solar activity varies with altitude and latitude. In the upper strat-

osphere, ozone during solar maximum is 2 to 5% higher than in solar minimum, with an uncertainty around 2% (McCormack and Hood, 1996; Steinbrecht et al., 2004a; Figure 3-19 of Chapter 3). Sensitivity studies by Cunnold et al. (2004) indicate that current estimates of the solar cycle effect on ozone are probably sufficiently accurate to allow the separation of halogen decrease-related ozone increases from solar cycle effects in the upper stratosphere. Recent data from 2004 and 2005, i.e., from the beginning of the solar minimum, confirm this result (Steinbrecht et al., 2006a).

The situation is less clear for total column ozone. Depending on latitude and location, total column ozone is between 2 and 10 Dobson units (DU) higher during solar maximum, both in observations and model simulations, with uncertainty ranging from 2 to over 5 DU (McCormack et al., 1997; Steinbrecht et al., 2006b; Reinsel et al., 2005). One reason for this large uncertainty in the magnitude of the solar cycle variation in total ozone is the fact that the two solar maxima before 1999-2003 coincided with large volcanic eruptions. It is difficult to separate the impacts of eruptions and solar cycle on observed ozone (Solomon et al., 1996). There were no major volcanic eruptions during the 1999-2003 solar maximum. However, in this case, the ozone response is contaminated by the ozone changes related to the turnaround of ODSs, that we are trying to quantify. It is further unlikely that the solar cycle signal in ozone exactly follows the simple proxies used in most analyses, such as the Mg II core-to-wing ratio, 10.7 cm radio flux, or an 11-year harmonic function (Steinbrecht et al., 2004a,b). The response may inherently vary from one solar maximum to the next (Ruzmaikin et al., 2003). All of the above factors add uncertainty to estimates of ozone increases in all three past solar maxima. In particular, they complicate the separation of recent or near-term increases in ozone due to the EESC turnaround from increases due to the 1999 to 2003 solar maximum. It is likely that observations at least to the end of the next solar minimum in 2008 will be required to allow better separation of solar cycle effects from possible ozone increases due to decreases in EESC.

6.3.6 Volcanic Eruptions

As discussed in the previous Ozone Assessment (WMO, 2003) and in Chapter 5, volcanic eruptions can have a large impact on stratospheric ozone by changing heterogeneous chemistry, thermal structure, and circulation in the stratosphere. Because of this, it is necessary to consider volcanic eruptions both when interpreting observed changes and when making projections of future changes of ozone.

There have been no large volcanic eruptions since the 1991 Mt. Pinatubo eruption, and the stratospheric aerosol loading in the four years since the previous Ozone Assessment has remained at low, nonvolcanic levels. However, the impact of the Mt. Pinatubo eruption still needs to be considered when attributing changes in ozone in the last decade of the 20th century to changes in ODSs (or any other factor). The Mt. Pinatubo eruption contributed to a large decline in Northern Hemisphere ozone, which was followed by an increase in ozone as stratospheric aerosols decayed back to low, nonvolcanic levels. This decrease in aerosol levels occurred at around the same time that the growth in EESC slowed and reached its peak value. Both the changes in aerosols and EESC led to changes in ozone levels, and it is difficult to separate their impact on ozone.

If one or more large volcanoes erupt in the next 50 years, it is likely to impact the ozone recovery process. The overall impact of volcanic eruptions varies with halogen levels (see Chapter 5). Outside the polar regions, the primary effect of an increased rate of heterogeneous reactions is to cause a reduction of nitrogen oxides. In the current high-chlorine conditions, this causes an increase in reactive chlorine and increased ozone depletion, as observed following the Mt. Pinatubo eruption (Brasseur and Granier, 1992). However, in low-chlorine conditions, a large volcanic eruption could cause a small ozone increase due to the suppression of nitrogen oxides (e.g., Tie and Brasseur, 1995). Hence, a large, Pinatubo-like eruption within the next 20 years, when there will still be significant amounts of halogens in the stratosphere, may lead to an increase in ozone destruction by ODSs and a temporary delay in ozone recovery; whereas a similar eruption in the more distant future, when EESC has decreased to around or below 1980 values, may lead to an increase in ozone levels. In both cases, the exact impact will depend on the latitude and size of the volcanic eruption, and ozone may also be impacted by changes in the stratospheric thermal structure and circulation caused by the eruption.

6.4 STATISTICAL METHODS FOR DETECTION OF MILESTONES

Detection of recovery milestones, and in particular the detection of the onset of ozone recovery (i.e., a slowing of the ozone decline), cannot be achieved simply by examining raw measurement time series. Statistical methods are required to distill the subtle changes in trend from an observed ozone time series. Typically, multiple linear regression fits are used with various proxies accounting for different contributions to the ozone variation, which

have been described in Section 6.3. Autocorrelation in the residual time series also needs to be considered (Tiao et al., 1990). Several different approaches have been used on model output, total column data, and vertically resolved data, to test the last few years of data for an increase in values: the change in linear trend ("change-in-trend") method (Reinsel et al., 2002), the multivariate adaptive regression splines method (Krzyścin et al., 2005), the flexible tendency method (Harris et al., 2001), or the cumulative sum of residuals (CUSUM) method (Reinsel, 2002; Newchurch et al., 2003). Each has its merits, offers slightly different information, and tests different hypotheses with the data. The change-in-trend and CUSUM approaches have been used extensively to examine recent data and test for early signs of changes in ozone trends. They are discussed in more detail below. Both of these methods assume linear trends in ozone between the start of the analysis period (usually 1980) and a selected "turnaround date" (usually 1996). Over this period, when EESC increased approximately linearly, the expectation is, therefore, that ozone loss is linearly proportional to EESC. This assumption has been shown to be valid over midlatitudes (Yang et al., 2006), over the Arctic (Douglass et al., 2006), and over the Antarctic when ozone destruction is incomplete (Jiang et al., 1996).

6.4.1 Change in Linear Trends

In the change-in-trend method (Reinsel et al., 2002), the standard least-squares regression model (see Chapter 3) is extended by adding a second basis function, set to zero before a selected turnaround date and proportional to time thereafter (Figure 6-2). The turnaround date is preselected and its choice can affect the results. Such a regression model gives an estimate of the magnitude of the trend before the turnaround date (m_1), the slope change at the turnaround date (m_2), and the magnitude of the trend after the specified turnaround date (m_1+m_2). The statistical significance of m_2 can be tested and a change-in-trend milestone is reached when m_2 is significantly different from zero at the 2σ level. This method assumes that the ozone record exhibits a discrete change from a downward trend to a less steep trend or an upward trend across the turnaround date (Reinsel et al., 2002). Calculations indicate that the actual shift from upward trend to downward trend in EESC may take a few years, but includes a near linear trend prior to the turnaround and a near linear trend for a few years after this turnaround (WMO, 2003). If the underlying trend in ozone follows this EESC pattern, the piecewise linear and contiguous approach may be appropriate. Each data point, in most cases monthly and regionally averaged data, is weighted by the square of the distance from the fit, resulting in large deviations having a strong influence on the final trend estimates. Anomalous years either near the turnaround or near the beginning or end of the record have particularly high leverage on the trend estimates.

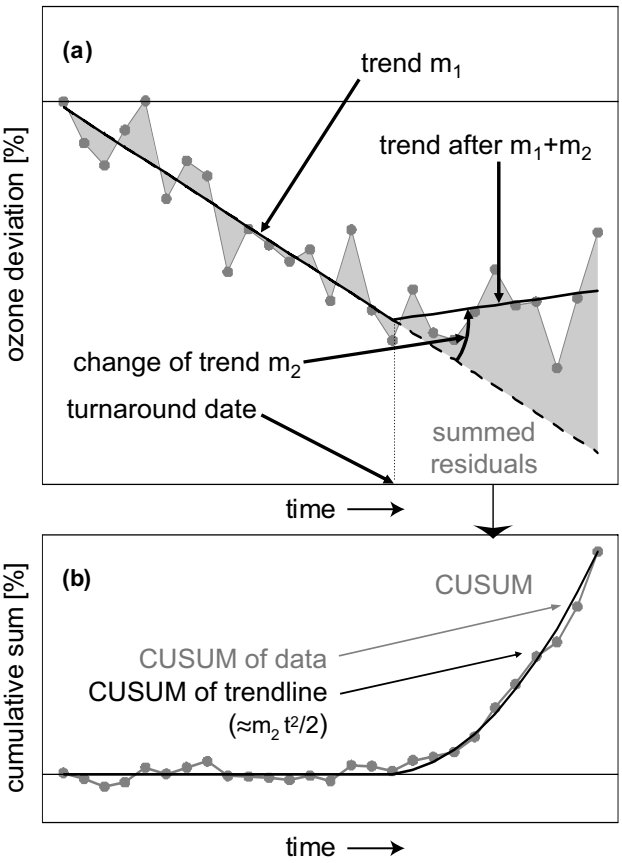

Figure 6-2. A schematic representation of (a) the change-in-trend method, and (b) the CUSUM method. See Section 6.4 for discussion.

6.4.2 Cumulative Sum of Residuals

The CUSUM approach (Reinsel, 2002; Newchurch et al., 2003) assumes that the data, after accounting for various non-ODS influences, follow a near-linear downward trend until some preselected specified date, analogous to the turnaround date of the change-in-trend method. After that date, all later data are evaluated to determine if they represent a likely deviation from that downward trend. This evaluation is made by examining the cumulative sum of residual deviations from the extrapolated trend after the specified point (see Figure 6-2). The choice of the turnaround date is not very important provided it is not too far from the physically appropriate point (e.g., the date at which EESC maximizes). In contrast to the change-in-

trend approach, CUSUM makes no assumptions about the temporal path of the deviation. Data shifts, gradual reductions in trend, and slow changes to an extrapolated trend are all detected. However, little information is provided on the temporal shape of a change. Because the cumulative sum of deviations is considered, as opposed to the minimum of the sum of the squares as in the change-in-trend method, highly unusual points are somewhat less influential. The explanatory variables, such as the QBO, solar cycle, and an underlying trend, are fit for the entire time series and removed from the data to create the monthly ozone residuals. These residuals are used to form the trend estimate calculated over the period up to the turnaround date and extrapolated thereafter for the CUSUM calculation.

The CUSUM approach detects arbitrary deviations from the extrapolated trend, whereas the change-in-trend method looks for a specific temporal path. Comparison between the change-in-trend and CUSUM approaches is possible using the fact that if there is a change of trend by m_2 per unit time, the CUSUM value after the turnaround increases with time approximately as $m_2 t^2/2$ (Yang et al., 2006). For example, a representative change of trend m_2 for total ozone at northern midlatitudes is 2 DU per year, or 0.166 DU per month (see Figure 6-4, panel b). When accumulated over 84 months from January 1997 to December 2004, this change of trend corresponds to a CUSUM value of 595 cumulative DU by the end of 2004. This compares very well with the CUSUMs given in panels (d) and (f) of Figure 6-3 for partial ozone columns. By the end of 2004, these CUSUMs amount to 250 and 350 DU, or 600 DU combined for the total column.

6.5 ATTRIBUTION OF THE RECENT BEHAVIOR OF OZONE

To attribute the recent changes in ozone to changes in ODSs, we require more than the observation of a slowing of the ozone decline or an increase in ozone. We require that the observed changes in ozone occur at approximately the right time to be associated with ODS concentrations, that the magnitude of change in ozone trend be of the appropriate magnitude expected due to changes in ODS concentrations, and that the latitudinal, altitudinal, and seasonal changes are in agreement with the changes expected due to a turnaround in ODS concentrations. Even if all of the above are observed, scientific judgment is involved in assessing whether the recent changes in ozone are appropriately linked with the changes in ODS concentrations. Scientific judgment in this assessment process takes into account statistical studies, a variety of models involving a range of appropriate assumptions, an understanding of the time scales of relevance in the atmosphere, possible uncertainties in mechanisms governing ozone concentrations, as well as uncertainties in available ozone measurements.

Attribution is fundamentally difficult because, as discussed in Section 6.3, many factors other than ODSs can affect ozone on time scales of a few years. The separation of these other factors from any underlying ODS signal in ozone is further complicated by the fact that the quantification of the many factors affecting ozone is uncertain, can be nonlinear, and involves feedbacks through a variety of mechanisms. Furthermore, attribution requires analyzing data with high natural variability and using models that cannot represent atmospheric processes at arbitrary degrees of spatial and temporal resolution. Several approaches have been used to assess whether the changes in ozone can be attributed to changes in ODSs. These include using statistical methods to separate effects of transport and temperature from chemical effects of ODSs, and modeling efforts to partition the past changes into those due to ODS changes and those due to known transport and temperature effects.

6.5.1 Upper Stratospheric Ozone

As described in Section 6.2, the first stage of the ozone recovery process is defined as a statistically significant deviation above the previous linear decline in ozone that must be attributable to changes in EESC. We expect that this stage of ozone recovery will be passed first in those regions of the atmosphere where ozone changes are most closely controlled by changes in EESC. One such region is the upper stratosphere, where the largest ozone decline due to gas-phase chemical reactions has been recorded (WMO, 2003) and where few factors other than gas-phase chemistry directly control ozone. Reinsel (2002) and Newchurch et al. (2003) showed that a statistically significant deviation in the ozone decline can be found in observations of ozone in this altitude region. This deviation is illustrated in Figure 6-3(a), which shows ozone residuals for northern midlatitudes and the altitude range from 35 to 45 km. Residuals were defined by subtracting the mean annual cycle and estimated variations due to the solar cycle and QBO. Up to about the end of 1996, ozone residuals closely followed a linear decline of approximately −7% per decade, and since then, this steep decline has not continued and ozone levels have been essentially constant or may have even increased. This behavior is quantified in Figure 6-3(b), where the CUSUMs from the extrapolated 1979 to 1996 trend are shown. The CUSUM increases with time since 1996, demonstrating that the residuals lie significantly above the

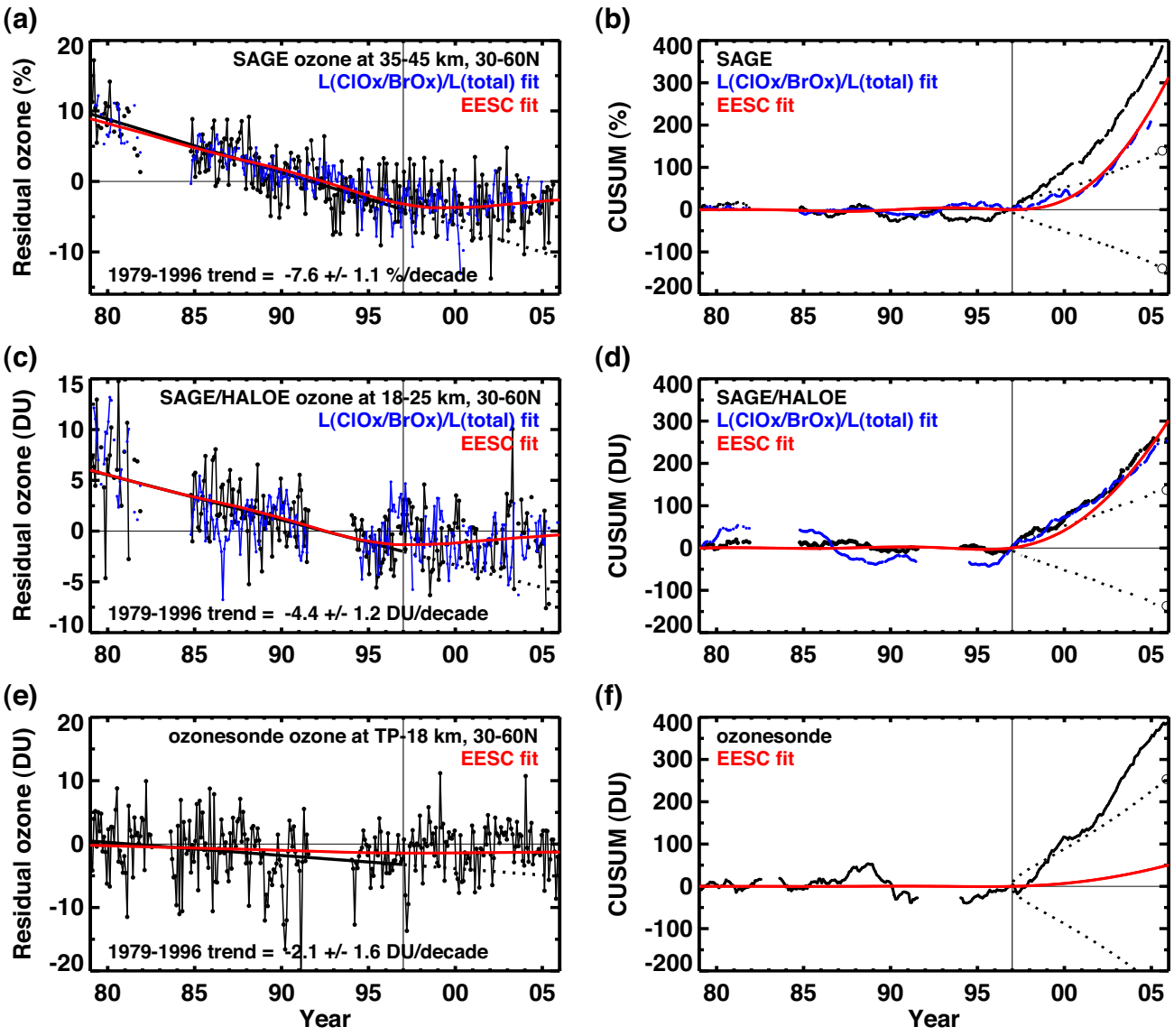

Figure 6-3. Time series of monthly average ozone residuals plus linear trend (left panels) and cumulative sum (CUSUM) of residuals (right panels) in percent or DU. Panels on the left show ozone column residuals between 30°N and 60°N, at 35-45 km from SAGE (top), at 18-25 km from SAGE and HALOE (middle), and from the tropopause (TP) to 18 km from ozonesondes (bottom). Ozone residuals, calculated over the period 1979-2005, have annual cycle, QBO, and solar cycle effects removed. In all left panels, EESC fits to the residuals are shown in red. The solid black lines on the left panels indicate the ozone trend calculated from observations for 1979-1996 and forecasted linearly afterward (dotted). The blue lines in the top and middle panels show the ozone evolution expected from photochemical model calculations. Cumulative sums of residuals of traces in the left hand panels are shown in the panels on the right together with the 95% confidence envelopes of departure from natural variability and model uncertainty as dotted lines. Updated from Newchurch et al. (2003) and Yang et al. (2006).

extrapolated trend line, and since about 1999 the CUSUM has exceeded the 2-sigma error envelope (95% confidence level) of a continuing decline. Similar behavior is found for equatorial latitudes and Southern Hemisphere midlatitudes (Newchurch et al., 2003).

The significant positive deviation of upper-stratospheric ozone levels from the previous linear decline shown in Figure 6-3(a,b) is corroborated by Petropavlovskikh et al. (2005) using Umkehr and SBUV(/2) data, and by Steinbrecht et al. (2006a) using

ground-based and satellite records for four stations between 45°S and 44°N and the change-in-trend method. The latter showed an increase in ozone residuals over the last few years for some of the stations (see also Figure 3-6 of Chapter 3). The lessening of the trends in the residuals depends to some degree on the estimates of the solar-cycle and QBO amplitude in ozone (Steinbrecht et al., 2004a; Cunnold et al., 2004), as discussed in Section 6.3. Also, the reduction in trend in upper stratospheric ozone was not significant at the most northerly station (48°N) considered by Steinbrecht et al. (2006a), see Figure 3-6. At northern midlatitudes, other unquantified factors seem to mask the reduction of the ozone decline expected from the beginning of the decline of EESC. A general problem is the lack of long-term upper stratospheric ozone records at latitudes north of 60°N. Nevertheless there is now conclusive evidence for a reduction in the negative trend in upper-stratospheric ozone over a wide region between southern and northern midlatitudes.

The observations of a slowing of the ozone decline discussed above do not alone constitute the first stage of recovery as these changes need to be attributed to changes in ODS amounts. While the ozone changes are in general consistent with those expected from changes in EESC, we recognize that we do not have a full quantitative understanding of ozone loss in the upper stratosphere (Chapter 3). The smooth curves in Figure 6-3(a,b) show fits to the ozone residuals using the EESC (red curve) and ozone loss fraction due to chlorine and bromine (blue curves). The latter was calculated using a photochemical model constrained by observations of total reactive nitrogen (NO_y), inorganic chlorine (Cl_y), CH_4, and H_2O (Yang et al., 2006). As quantified by the CUSUMs, these fits show a significant deviation from the previous decline up to 1997. The good fit to the observed ozone residuals by 1) EESC and 2) the calculated ozone loss fraction due to EESC, as well as the fact that most other sources of ozone variability have been removed, provides strong evidence that the slowing of the ozone decline in the midlatitudes in the upper stratosphere can be attributed to changes in ODSs.

6.5.2 Lower Stratospheric and Total Column Ozone

A similar slowing of the decline since 1997 has also been observed in total column ozone, and in some regions of the globe, column ozone has even increased since 1997 (Chapter 3). This deviation from the previous decline is, in general, statistically significant (e.g., Reinsel et al., 2005; Krzyścin et al., 2005; Dhomse et al., 2006; Miller et al., 2006; Krzyścin, 2006; Yang et al., 2006).

The change in total column ozone evolution is illustrated in Figure 6-4, which shows calculations of the overall trend and the change in trend (see Section 6.4) of column ozone as a function of latitude (Reinsel et al., 2005). The change-in-trend term is statistically significant at the 95% confidence level between 40°N and 60°N, and between 50°S and 60°S. At lower latitudes the change in trend is not statistically significant. The trends and changes in trends shown in Figure 6-4 are representative of the range of results obtained in Chapter 3 for various total column ozone datasets. Furthermore, several other studies (Krzyścin et al., 2005; Dhomse et al., 2006; Krzyścin, 2006; Yang et al., 2006) came to a similar conclusion based, in part, on additional data and using somewhat different approaches. A statistically significant slowing of the decline is also found for ozone in different altitude regions. For example, Figures 6-3(c) and (e) show residuals for ozone between 18 and 25 km and between the tropopause and 18 km, respectively. The corresponding CUSUMs (Figures 6.3(d) and (f)) indicate a similarly significant deviation from the previous decline.

The above studies have shown that there is now substantial evidence that a slowing of ozone decline has occurred not only for upper stratospheric ozone (Section 6.5.1), but also for lower-stratospheric and total column ozone over substantial parts of the globe. However, it is still necessary to attribute these ozone deviations to changes in EESC in order to label this as stage (i) of ozone recovery. This attribution can be done by estimating changes in chemical ozone destruction (Yang et al., 2006), by eliminating as many non-chemical ozone variations as possible (e.g., Hadjinicolaou et al., 2005; Reinsel et al., 2005; Miller et al., 2006; Dhomse et al., 2006), or by comparisons with multidimensional models (e.g., Anderson et al., 2006; Weatherhead and Andersen, 2006).

Yang et al. (2006) compared the changes in ozone residuals for column ozone, ozone between 18 to 25 km, and ozone between the tropopause and 18 km with changes in EESC and those in the chemical ozone loss fraction due to chlorine and bromine (using the same model as described in Section 6.5.1). As shown in Figures 6-3(c) and (d), the ozone residuals in the 18 to 25 km altitude range closely follow both the EESC and the model-calculated ozone loss fraction due to chlorine and bromine, and CUSUM calculations indicate statistical significance above the 95% confidence level. This result is robust for both northern and southern midlatitudes. It is a strong indication that the beginning of the reduction in EESC is mirrored in photochemical ozone loss rates and that this is the major contributor to the recent leveling off of ozone residuals in the 18 to 25 km range (Yang et al., 2006). The situation is however different for the lower altitude range

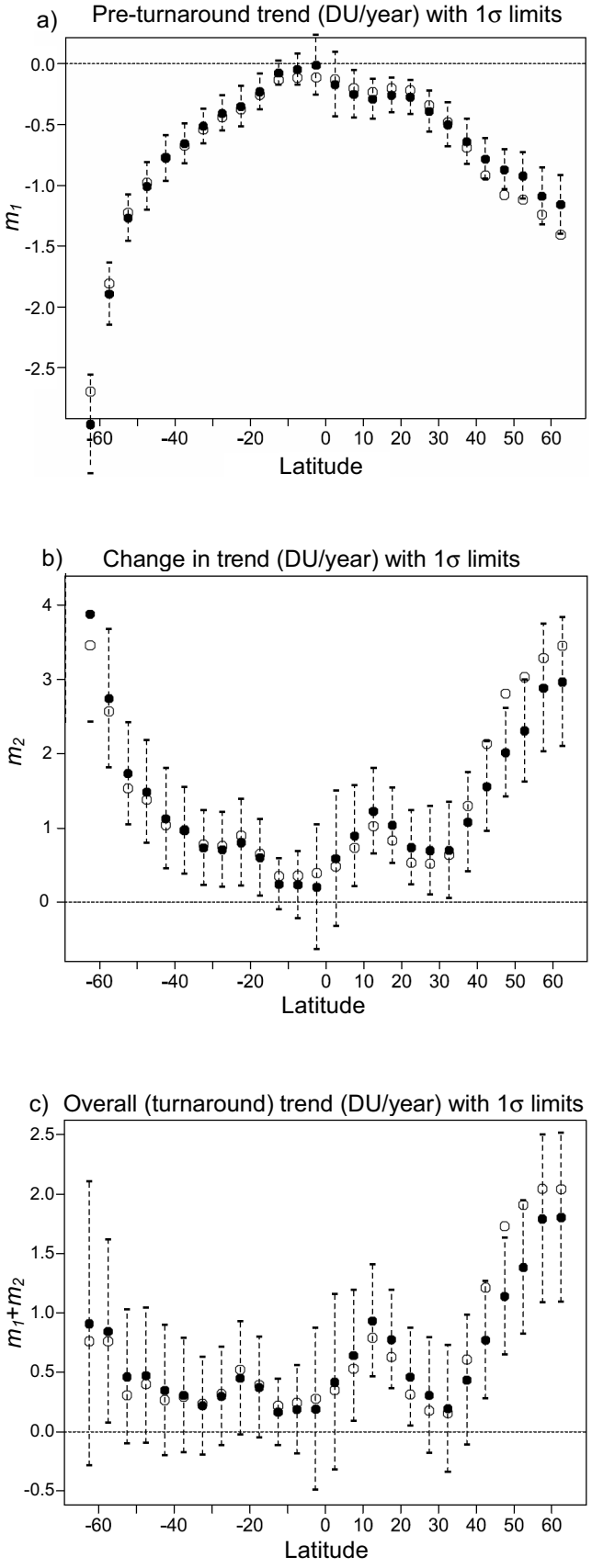

from the tropopause to 18 km (Figure 6-3(e) and (f)). Although ozone residuals between the tropopause and 18 km have increased, the low cumulative sum of residuals for the EESC fit (red curve in Figure 6-3(f)) suggests that these changes have not been driven by declining EESC. Because ozone is significantly controlled by transport in this region, the low CUSUM for EESC indicates that dynamical and transport changes likely account for the major part of the ozone increases between the tropopause and 18 km.

The altitude partitioning of total column ozone changes before and after 1997, according to Yang et al. (2006), is summarized in Table 6-2. About 80% of the total ozone decline between 1979 and 1996 occurred above 18 km, and, as discussed above, this is largely due to increasing EESC. The remaining 20% of the total ozone decline occurred below 18 km, where transport changes played a major role. For the recent total ozone increases, however, only about half comes from altitudes above 18 km, and can be attributed to changes in EESC. The other half comes from altitudes between the tropopause and 18 km, and must largely be due to dynamical and transport changes. The error bars on this partitioning are substantial, of the order of ±30%; nonetheless, the CUSUM statistics are well above the 2σ level.

Numerous other studies, using a variety of approaches, have also concluded that changes in transport make a major contribution to the recent increase of total column ozone. Multilinear regression studies by Dhomse et al. (2006), Reinsel et al. (2005), or Krzyścin (2006) show that dynamical factors account for a major fraction, but not all, of the recent increases in total ozone. Figure 6-4, for example, indicates that for northern lati-

Figure 6-4. Trends in zonal mean (5°) total column ozone from the merged Total Ozone Mapping Spectrometer/Solar Backscatter Ultraviolet spectrometer (TOMS/SBUV) satellite dataset (see Chapter 3). (a) Pre-turnaround trends calculated over the period 1979-1996; m_1 as shown in Figure 6-2. (b) The change in trend at the turnaround date, calculated using data over the period 1979 to 2002; m_2 as shown in Figure 6-2. (c) the overall trend; $m_1 + m_2$ as shown in Figure 6-2. All trends are shown with 1σ error bars. Trends from a regression model incorporating basis functions to account for changes in ozone driven by the Arctic Oscillation, Antarctic Oscillation, and wave activity are shown using filled circles, while trends calculated using a traditional regression model incorporating trend, QBO, and solar cycle terms are shown using open circles. From Reinsel et al. (2005).

Table 6-2. Total column ozone trends and trend changes, and contributions from different altitude ranges. The column ozone is obtained from the Dobson/Brewer (total), Stratospheric Aerosol and Gas Experiment (SAGE) satellite (above 25 km), SAGE (18 to 25 km), and ozonesonde (tropopause (TP) to 18 km) measurements. The fractions with respect to the ozone column above the tropopause are listed in percent. Results are for the 30° to 60°N latitude band. Uncertainties given are 2σ. Adapted from Yang et al. (2006).

Altitude Range	Trend 1979-1996 (DU/decade)	Fraction of Total Trend 1979-1996 (%)	Change of Trend 1997-2005 (DU/decade)	Fraction of Change of Trend 1997-2005 (%)
Total column	–8.7 ± 2.3		17.4 ± 8.2	
Above 25 km	–4.3 ± 1.0	42 ± 10	4.9 ± 2.9	30 ± 18
18 to 25 km	–3.9 ± 0.9	38 ± 9	3.4 ± 2.8	21 ± 17
TP to 18 km	–2.1 ± 1.6	20 ± 16	8.0 ± 5.3	49 ± 3

tudes, trends before and after 1996 are comparable in magnitude. Since EESC is declining at a rate three times slower than the previous increase, this is a strong indication for a major contribution from transport to the post-turnaround trend, at least in the Northern Hemisphere. Chemical transport model simulations using the European Centre for Medium-Range Weather Forecasts ERA 40 meteorological reanalyses with chlorine fixed at 1980 levels can reproduce the total ozone increase from 1996 to 2003 (Hadjinicolaou et al., 2005; see also Chapter 3). Analysis of Canadian ozonesondes indicates significant increases in ozone below 60 hPa (20 km), mostly related to dynamical changes in the occurrence of ozone laminae (Tarasick et al., 2005). Furthermore, studies suggest that changes in the mean meridional Brewer-Dobson circulation, e.g., inferred by 100 hPa Eliassen Palm flux, and in lower tropospheric wave forcing, e.g., described by potential vorticity, can account for a substantial fraction of the pre-1997 total ozone decline outside the polar regions and also for the recent increases in northern midlatitude spring (e.g., Salby and Callaghan, 2004; Malanca et al., 2005; Hood and Soukharev, 2005; see also Section 3.4.2 of Chapter 3).

Andersen et al. (2006) compared the recent changes in total column ozone with fourteen 2-D and 3-D model estimates of recovery rates. The comparison showed that for most areas, the changes in long-term trends were in agreement with the range of model expectations for the long-term trends. However, the change in trend was larger than any of the models predicted for the same short time period (1996-2003). In particular, they showed that the large changes observed in the high northern latitudes were larger than any of the models predicted, indicating that much of the change observed north of 50°N may be natural variability and such trends will not continue into the future at the same rate. Weatherhead and Andersen (2006) extended this analysis and showed that the latitudinal, altitudinal, and seasonal signatures of change in ozone from 1996 through 2005 are in rough agreement with what models are predicting for long-term ozone change (between 1996 and 2050 for the 2-D models and for periods of time-slice runs for 3-D models); see Figure 6-5. The models and measurements agree well in the Southern Hemisphere, and in the Northern Hemisphere show rough agreement for past trends but significant disagreement for the magnitude of trends since 1996. Some of this disagreement could be due to the different time periods considered for observations and models.

All of the above approaches suffer from methodological and statistical uncertainties. Multilinear regression methods are limited by the simplicity of the underlying assumptions, and are only an attempt to describe very complex processes in the atmosphere with a simple set of indices. Not all effects, e.g., solar cycle effects, may be correctly removed on the basis of these simple indices. The reconstruction of chemical ozone loss may require substantial data extrapolation to include periods before measurements of key species (e.g., methane) were available (Yang et al., 2006). Also, bromine may be more important in the lower stratosphere, and lead to higher ozone loss than previously thought (Salawitch et al., 2005). Estimations on the basis of chemical transport models and reanalysis datasets (National Centers for Environmental Prediction (NCEP) or ERA-40), e.g., Hadjinicolaou et al. (2005), suffer from uncertainty regarding the long-term consistency of the reanalysis datasets and their ability to correctly describe the slow mean meridional circulation (see Chapter 3). Also, the meteorological data may inherently contain effects from

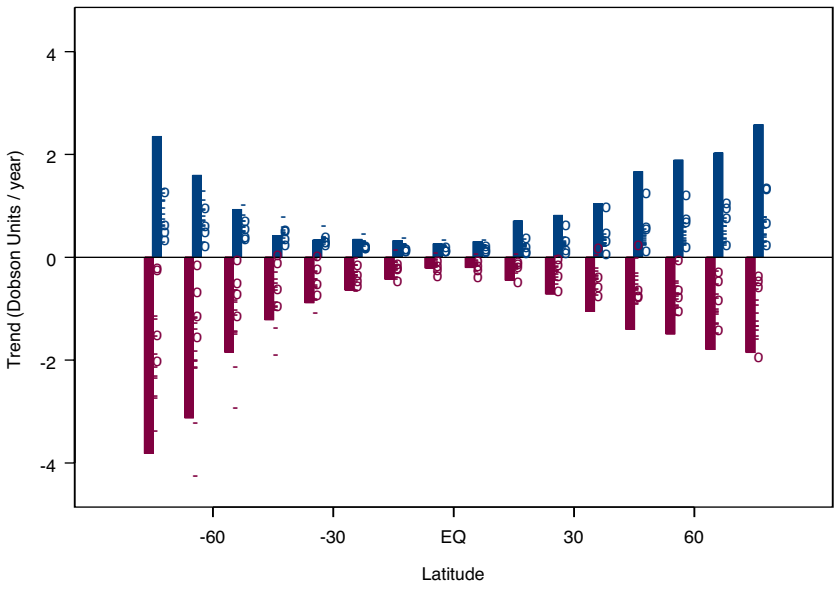

Figure 6-5. Measured and modeled column ozone trends by latitude for 1979-1995 (in red) and 1996-2005 (in blue). Increases in ozone during the past eight years coincide with the regions in which past depletion has occurred. Analyses of the measurements are represented by the solid bars; analyses of 2-D models are shown with horizontal dashes, and results of 3-D models are shown with circles. The model estimates for 1979-1995 are shown in red; projections for long-term recovery are shown in blue. Trends before 1995 are statistically significant (2σ) for middle and high latitudes. Data are from version 8 of the merged TOMS/SBUV2 dataset. Eq., equator; negative latitudes are degrees south. From Weatherhead and Andersen (2006).

the true ozone changes, making it difficult to separate chemical and transport processes.

Even though all approaches have uncertainties, the complementary approaches come to similar conclusions: that changes in transport have contributed a major fraction to the leveling off and increase in midlatitude total ozone since 1997, particularly in the lower stratosphere over northern midlatitudes. However the changes in trends are in agreement, on a number of criteria, with changes in EESC. It is likely that we have passed the "slowing of ozone decline" stage for total ozone over large parts of the globe and in the middle and upper stratosphere. However, at this time, due to the described statistical and methodological uncertainties, an unambiguous attribution to changes in EESC, with a high level of confidence, is not possible.

6.5.3 Polar Ozone

The sustained increase in the severity of Antarctic ozone depletion from the early 1980s to the later 1990s has not continued. Recent changes in metrics of the severity of Antarctic ozone depletion have ranged from little or no change over the past 10 years (ozone hole area), to small (minimum ozone levels) and moderate (ozone mass deficit) signs of ozone increases (Bodeker et al., 2005; Section 4.3.2 and Figure 4-8 of Chapter 4). The cessation of ozone hole growth can be ascribed to the fact that at current ODS levels, all or most of the ozone is destroyed between 12 and 24 km (e.g., WMO, 2003). Recent reductions in Antarctic ozone loss can be explained by anomalously high stratospheric temperatures and reduced frequency of PSCs in recent years (Solomon et al., 2005; Hoppel et al., 2005). Therefore, although recent stabilization and reduction of Antarctic ozone depletion has occurred at approximately the same time as the growth in EESC has slowed and passed its peak, this ozone change cannot be attributed solely to changes in EESC. It is therefore not possible to conclude that either the first or second stage of Antarctic ozone hole recovery has occurred. The near total destruction of ozone inside the ozone hole means that there is low sensitivity to moderate reductions in EESC. ODS amounts in the Antarctic vortex are expected to decrease only slowly over the next decade (polar EESC is decreasing at around 0.6%/year, see figure in Box 8-1 of Chapter 8). Therefore, in the near future, only small changes in Antarctic ozone area are expected as EESC declines, and these changes will be masked by interannual variability due to temperature and transport variations (Newman et al., 2004; Solomon et al., 2005).

Larger sensitivity to changes in EESC is expected at the upper altitudes of the ozone hole (20-22 km) where ozone depletion is not complete, and this has been identified as a possible region to detect Antarctic ozone recovery (Hofmann et al., 1997). Hoppel et al. (2005) analyzed measurements of ozone mixing ratios in the 20-22 km altitude range for October, and showed that the values for 2001-2004 were higher than for 1994-1996 and 1998-

2000. However, the higher ozone mixing ratios were accompanied by higher temperatures and reduced frequency of PSCs. Although ozone is more sensitive to ODS changes in the 20-22 km region, there is more dynamical activity in this region, and changes in ozone due to ODS changes cannot be clearly distinguished from those due to changes in meteorological conditions. It is therefore not possible to conclude that the first (or second) stage of ozone recovery has occurred at 20-22 km in the Antarctic.

Another region where detection of the first stages of ozone recovery may be possible is the polar vortex collar region (60°S to 70°S). Yang et al. (2005) examined the evolution of ozone in this region using several different datasets. They accounted for dynamical variability using the observed correlation between ozone and 100 hPa temperatures, and showed that temperature-adjusted ozone anomalies were roughly constant since 1997 (see Figure 6-6). The change in the trend of these anomalies is significant at greater than 95% confidence limits. Yang et al. also showed that complete ozone loss is infrequent in the collar region and was not responsible for the slowing of the ozone decline. As shown in Figure 6-6, the variation in the ozone anomalies is similar to that of midlatitude EESC, and fits to EESC can explain most of the long-term variations in the ozone anomalies. This high correlation and the limited role of complete ozone loss provide evidence that the first stage of ozone recovery may have occurred in the stratospheric collar region surrounding the Antarctica vortex. However, there is some uncertainty in the EESC in the collar region, and the resulting fit with temperature-adjusted ozone anomalies. For example, the polar EESC shown in Box 8-1 continues to increase until

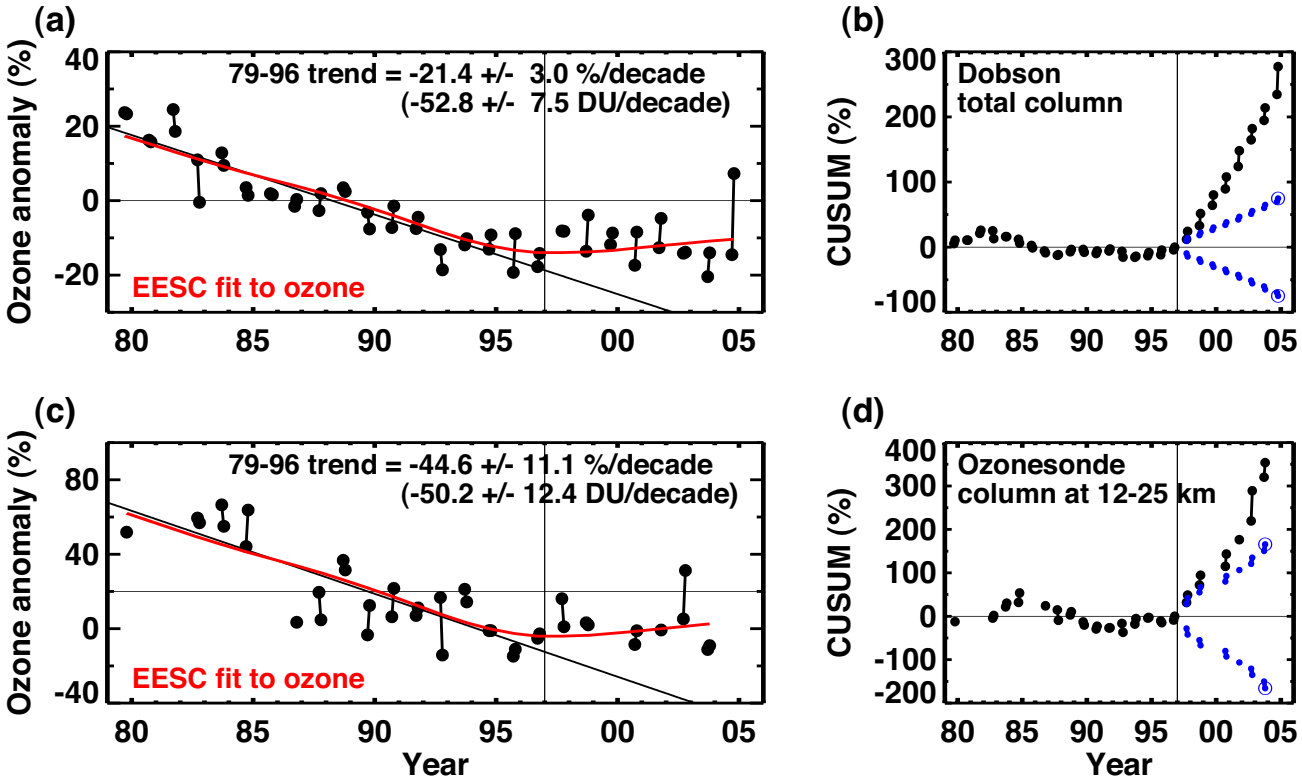

Figure 6-6. September and October temperature-adjusted ozone monthly anomalies (left panels) and CUSUM of ozone residuals (right panels) in percent for Dobson spectrophotometer total ozone columns at Vernadsky (65°S) and Syowa (69°S) (top) and ozonesonde ozone columns from 12-25 km at Syowa (bottom). The ozone anomalies are calculated from a regression model fit to the data over the full period. The temperature-adjusted ozone anomalies are obtained by subtracting the ozone equivalent temperatures from the ozone anomalies (see Yang et al., 2005, for details). The black line indicates the ozone trend calculated from observations for 1979-1996 and forecasted linearly afterward. Linear trends and 95% confidence intervals for 1979-1996 are listed in %/decade and DU/decade. The red line shows the EESC fits to the temperature-adjusted ozone. The blue lines indicate the 95% confidence envelopes of departure from natural variability and trend model uncertainty. Adapted from Yang et al. (2005).

2001, in contrast to the ozone anomalies in the collar that peak around 1997. It is unclear whether the midlatitude or polar EESC is more representative for the collar region which is outside the ozone hole. These uncertainties cast some doubt on using EESC to quantify the role of ODSs in the stabilization of ozone in the collar region.

The expected slow improvement of Antarctic ozone over the next decade (e.g., Newman et al., 2004, 2006) means that variability will continue to complicate detection of the first and second stages of ozone hole recovery, even after accounting for temperature variations. Solomon et al. (2005) have suggested that the return of (1) the relationship between temperature and ozone and (2) the variance in ozone abundances to historical values may provide early signals of the beginning of recovery inside the ozone hole. However, after a stage of recovery has occurred, it is unclear how long it will take to achieve the detection of the stage using either diagnostic.

The issue of identifying recovery in the Arctic springtime is even more difficult than in the Antarctic. Arctic ozone depletion occurs in most years, but there is substantial interannual variability (see Chapter 4). The larger meteorological variability in the Arctic compared with the Antarctic (e.g., Langematz and Kunze, 2006) and smaller ozone depletion means that it will likely take many years to detect any changes in ozone due to decreases in EESC. Furthermore, it is likely that the first stage of recovery (slowing of decline) cannot be detected for the Arctic. As with the Antarctic, the first signals of recovery might be found by looking at the relationship between ozone and temperature. As discussed in Chapter 4, one relationship that reduces the variability is the compact relationship between vortex average ozone loss and V_{PSC}, the volume of air potentially containing PSCs (Rex et al., 2004). It may be possible to detect the recovery of polar ozone in the Northern Hemisphere from a statistically significant and persistent deviation from this relationship. However, no such deviation has been detected, and there has been no detection of any ozone recovery stages in the Arctic.

6.6 PROJECTIONS OF THE FUTURE BEHAVIOR OF OZONE

As discussed above (and in Chapter 5), the process of recovery of the ozone layer will depend not only on the decline of ODSs but also on many other factors. Although some of these factors can be accounted for empirically when projecting future ozone (e.g., Knudsen et al., 2004), coupling between the different chemical, dynamical, and radiative processes involved requires the use of models that include these interdependencies to make well-founded projections. In particular, models used for prognostic studies should incorporate the effects of changes in temperature and transport that are likely to occur as the concentrations of WMGHGs rise. This section addresses how changes in ODSs couple with other atmospheric changes to influence the long-term evolution of ozone.

The framework introduced in Section 6.2 is used to examine the ozone recovery process in the model simulations. In particular, projections of total column ozone are examined for three periods:

(i) The beginning of the century (2000-2020), when EESC is expected to start to decrease or continue to decrease
(ii) Mid-century (2040-2050 in extrapolar regions, 2060-2070 in polar regions), when EESC is expected to fall below 1980 values
(iii) End of the century (2090-2100), when factors other than ODSs are expected to control stratospheric ozone

Confidence in projections near the beginning of the century is higher than near the middle or end of the century because the former can be supported by observations, empirical studies, and extrapolations while the latter are more influenced by uncertainties in the emissions scenarios and other boundary conditions. In general, a separation of the different factors contributing to the ozone variability in the model output has not been performed. Therefore the modeled ozone time series presented below cannot be used for attribution of ozone changes to changes in ODSs.

6.6.1 Model Descriptions and Scenarios

In this Assessment both two-dimensional chemical transport models (2-D models) and three-dimensional coupled Chemistry-Climate Models (CCMs) are used to make projections of the ozone layer in the 21st century. By using both classes of models, with their respective advantages and disadvantages, the conclusions drawn from the model projections are likely to be more robust.

2-D models have been used extensively in previous Assessments. Their relative computational efficiency allows long integrations and a large number of sensitivity studies. This capability makes these models a valuable tool for understanding and quantifying the long-term changes in ozone. However, due to the inherent zonal averaging within these models, they are not well suited for modeling polar processes. The 2-D models used in this Assessment (see Table 6-3 for a summary of their characteristics) vary in the extent to which they incorporate interactions between model components. Most of the 2-D models use prescribed temperatures and transport, and therefore do not include the well-known temperature feed-

Table 6-3. A summary of the 2-D models used in this chapter.

Model	Institution(s)	Investigators	Temperature	PSC Scheme	Solar Cycle	Reference
AER	AER, Inc., U.S.	D. Weisenstein	Specified from NCEP analyses	Based on model T	No	Rinsland et al. (2003)
GSFC-INT	NASA/Goddard Space Flight Center	E. Fleming, C. Jackman	Interactive	Based on observed T	No	Rosenfield et al. (1997)
GSFC	NASA/Goddard Space Flight Center	E. Fleming, C. Jackman	Specified from UKMO analyses	Distribution based on NCEP	No	Fleming et al. (1999)
Leeds-Bremen	University of Leeds, U.K.; University of Bremen, Germany	M. Chipperfield, M. Sinnhuber, B.-M. Sinnhuber	Interactive	Based on model T	No	Chipperfield and Feng (2003)
MNP [1]	Netherlands Environmental Assessment Agency	G. Velders	Climatology	No solid PSCs	No	Velders (1995)
MPIC	MPI for Chemistry, Mainz, Germany	C. Brühl	Specified from CIRA data	Based on model and observed T deviation	No	Grooß et al. (1998)
NOCAR	NOAA/NCAR	R. Portmann	Interactive	Based on NCEP T, Liquid aerosols	No	Portmann et al. (1999)
OSLO	University of Oslo, Norway	B. Rognerud	Specified	Based on climatology	No	Stordal et al. (1985); Isaksen et al. (1990)
SUNY	SUNY, U.S.; St. Petersburg, Russia	S. Smyshlyaev	Specified from NCEP analyses	Based on NCEP T	Yes	Smyshlyaev et al. (1998)

AER, Atmospheric and Environmental Research Inc.; MPIC, Max-Planck Institute for Chemistry; NOAA, National Oceanic and Atmospheric Administration; NCAR, National Center for Atmospheric Research; SUNY, State University of New York; NCEP, National Centers for Environmental Prediction; UKMO, United Kingdom Meteorological Office; CIRA, COSPAR (Committee on Space Research) International Reference Atmosphere.

[1] This was referred to as the RIVM model in the 2002 Ozone Assessment (WMO, 2003).

back from changes in WMGHGs, or the ozone radiative-dynamical feedback, in which changes in ozone also affect the radiative balance of the stratosphere and hence temperatures and transport. Three of the models (NOCAR, Leeds-Bremen, and GSFC-INT) calculate temperatures from the modeled atmospheric composition, and capture some of the feedback on the circulation and transport. However, these so-called "interactive" models do not include changes in the wave forcing.

CCMs have a much more limited history in the Ozone Assessments. WMO (2003) was the first time CCMs were fully integrated into an Assessment. These simulations focused on the polar regions and, due to computational limitations, were largely restricted to the recent past and near future (roughly 1980 to 2020). Transient simulations (see Box 5-1 in Chapter 5) are preferred for predicting future ozone because in these simulations, ozone responds interactively to the gradual secular trends in WMGHGs, ODSs, and other boundary conditions. For this Assessment we consider only transient simulations from CCMs, and we examine global as well as polar ozone. Since WMO (2003), several new CCMs have been devel-

oped, significantly deepening the pool of model simulations of future ozone.

An additional improvement over the approach used in WMO (2003) is the use of two standard simulations, defined as part of the CCM Validation Activity (CCMVal; Eyring et al., 2005). One "past" simulation (REF1) is designed to reproduce ozone changes from 1980 to the present when global ozone observations are available. It allows a detailed investigation of the role of natural variability and other atmospheric changes important for ozone trends. All forcing fields in this simulation are based on observations (Appendix 6A). The "future" simulation (REF2) is a self-consistent simulation from the past into the future. In this simulation the surface time series of halocarbons is based on the "Ab" scenario from WMO (2003); see Appendix 6A. The new halogen scenario A1 from this Assessment (Chapter 8) has not been applied because the computational requirements of the CCMs meant that these simulations had to be started well before the scenarios in Chapter 8 were finalized. The WMGHG concentrations for the future simulations are taken from the IPCC (2000) "A1B" scenario, while sea surface temperatures (SSTs) are taken from different coupled ocean model simulations, either from simulations with the ocean coupled to the underlying general circulation models, or from the U.K. Meteorological Office HadGEM1 simulations using IPCC (2000) scenario "A1B." Some CCMs ran multiple future simulations with the same boundary conditions but different initial conditions (see Table 6-4). In general, the variability between ensembles from a single model is much smaller than the inter-model differences (see also Austin and Wilson, 2006; Dameris et al., 2006).

For consistency, the 2-D model simulations used the same halogen and WMGHG scenarios as the CCMs. Additional sensitivity runs with different scenarios were also performed by some 2-D models (see discussion below and Table 6-3). In this chapter, the focus is on the "future" simulations out to 2100, whereas the "past" simulations (up to 2004) are discussed in Chapter 3. Of the 13 CCMs available (see Table 6-4 for a summary of their characteristics), all but UMETRAC and LMDZrepro provided simulations of future ozone changes, and their results form the basis for the projections discussed in Sections 6.6.3 and 6.6.4.

6.6.2 Model Evaluation

Most of the 2-D models listed in Table 6-3 have been used in earlier Assessments. Their use in the past has often been accompanied by model intercomparisons and comparisons with measurements to characterize their capabilities and deficiencies. For example, Park et al. (1999) assessed the chemistry and transport in a large number of 2-D and 3-D chemical transport models (CTMs) (including the AER, GSFC-INT, GSFC, and NOCAR 2-D models considered here). This study showed that there was a large variation in the transport in the models, and most models produced air that was too young in the stratosphere and did not correctly simulate the tropical "tape recorder" (Mote et al., 1996). Also, there were significant differences in the NO_y and Cl_y in the lower stratosphere. Here, 2-D models are used to predict ozone changes in the midlatitudes and tropics. More emphasis has been given to interactive 2-D models because non-interactive 2-D models neglect the important effects of temperature feedback from changes in WMGHGs and the ozone radiative-dynamical feedback.

An evaluation of the CCMs used here is reported in Eyring et al. (2006). They compared simulations of the recent past (1960 to 2004) with meteorological analyses and trace gas observations. This CCM evaluation provides guidance on the level of confidence that can be placed on each model simulation.

The comparisons in Eyring et al. (2006) showed that the models reproduce the global, annual mean temperature fairly well, but most CCMs still have a cold bias in winter-spring in the Antarctic resulting in later polar vortex breakup (most severe in LMDZrepro and E39C). Most models display the correct stratospheric response to wave forcing in the Northern Hemisphere, but in the Southern Hemisphere several of the models (e.g., CCSRNIES, E39C, MAECHAM4CHEM, MRI, LMDZrepro, and ULAQ) have temperatures that are rather unresponsive to changes in the heat fluxes, with the ULAQ model having the incorrect sign. These biases indicate problems in the simulation of the dynamical response of the Southern Hemisphere stratosphere in winter in these models.

Eyring et al. (2006) also evaluated the transport in the CCMs by comparing simulated methane, mean age of air, and the water vapor "tape recorder" with observations. They found a wide spread in the model results for each diagnostic, indicating large differences in the transport. However, the majority of the spread is due to only a small subset of models (E39C, MAECHAM4CHEM, MRI, SOCOL, and ULAQ) where large deviations from observations are apparent in several, if not all, of the transport diagnostics. This is illustrated for methane and mean age of air at 50 hPa in Figure 6-7(a) and (b), where the above models are shown as dashed curves. The cause of significant biases in the tracer fields in these models is generally not known, but in some cases it can be attributed to specific model

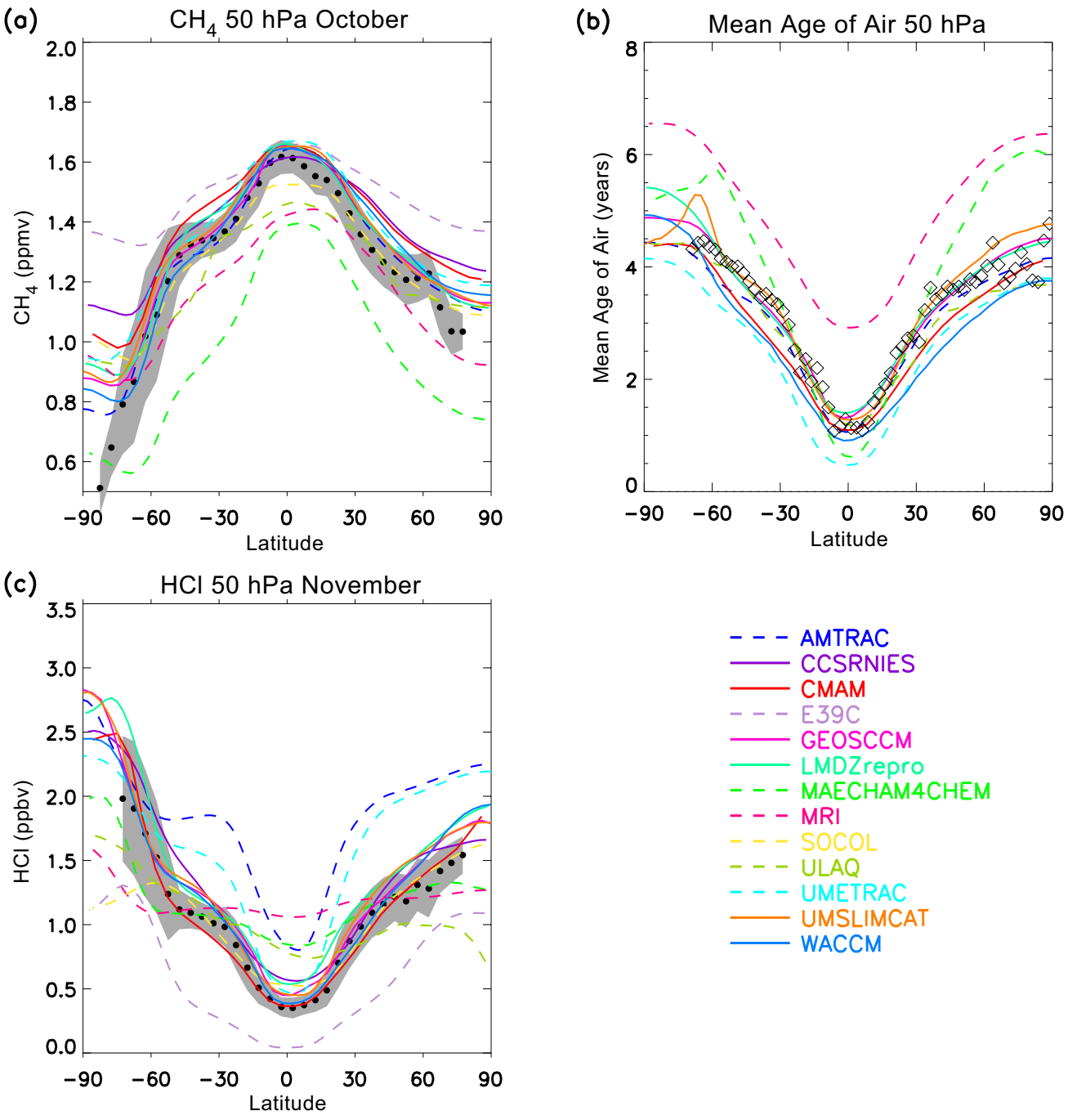

Figure 6-7. Comparison of climatological zonal-mean (a) methane in October, (b) annual mean of the mean age of air, and (c) HCl in November, at 50 hPa from CCMs and observations. Observations in (a) and (c) are from HALOE: Black dots are values averaged in latitudes (zonal means) and the gray area shows plus and minus 1 standard deviation about the climatological zonal mean HALOE. Observations in (b) are based on ER-2 aircraft measurements of CO_2 from many different years and months (Andrews et al., 2001). Adapted from Eyring et al. (2006).

Table 6-4. A summary of the CCMs used in this Assessment. See Appendix 6A for descriptions of the model runs. All CCMs have a comprehensive range of stratospheric chemical reactions, except E39C and MAECHAM4CHEM, which do not include bromine chemistry.

Model	Institution(s)	Investigators	Horizontal Resolution	No. Levels/ Upper Boundary	Runs	Reference
AMTRAC	GFDL, U.S.	J. Austin R. Wilson	2° × 2.5°	48 / 0.0017 hPa	3×REF1[a] 3×SCN2[b]	Austin et al. (2006); Austin and Wilson (2006)
CCSRNIES	NIES, Tsukuba, Japan	H. Akiyoshi T. Nagashima M. Yoshiki	2.8° × 2.8° (T42)	34 / 0.01 hPa	REF1 REF2	Akiyoshi et al. (2004); Kurokawa et al. (2005)
CMAM	MSC, Univ. of Toronto and York Univ., Canada	J. McConnell N. McFarlane D. Plummer J. Scinocca T. Shepherd	3.75° × 3.75° (T32)	71 / 0.0006 hPa	3×REF2[e]	Beagley et al. (1997); de Grandpré et al. (2000)
E39C	DLR Oberpfaffenhofen, Germany	M. Dameris V. Eyring V. Grewe M. Ponater	3.75° × 3.75° (T30)	39 / 10 hPa	3×REF1 4×SCN2 2×NCC	Dameris et al. (2005, 2006)
GEOSCCM	NASA/GSFC, U.S.	A. Douglass P. Newman S. Pawson R. Stolarski	2° × 2.5°	55 / 0.01 hPa	REF1[c] REF2	Bloom et al. (2005); Stolarski et al. (2006)
LMDZrepro	IPSL, France	S. Bekki F. Lott F. Lefèvre M. Marchand	2.5° × 3.75°	50 / 0.07 hPa	REF1 REF2	Chemistry part: Lefèvre et al. (1994)
MAECHAM4 CHEM	MPI Mainz, Hamburg, Germany	C. Brühl M. Giorgetta E. Manzini B. Steil	3.75° × 3.75° (T30)	39 / 0.01 hPa	REF1 REF2 SCN2	Manzini et al. (2003); Steil et al. (2003)
MRI	MRI, Tsukuba, Japan	K. Shibata M. Deushi	2.8° × 2.8° (T42)	68 / 0.01 hPa	REF1 REF2	Shibata and Deushi (2005); Shibata et al. (2005)
SOCOL	PMOB/WRC and ETHZ, Switzerland	E. Rozanov M. Schraner	3.75° × 3.75° (T30)	39 / 0.01 hPa	REF1 REF2	Egorova et al. (2005); Rozanov et al. (2005)
ULAQ	Univ. of L'Aquila, Italy	E. Mancini G. Pitari	10° × 22.5°	26 / 0.04 hPa	REF1[d] REF2 NCC	Pitari et al. (2002)
UMETRAC	Met Office, U.K.; NIWA, New Zealand	N. Butchart H. Struthers	2.5° × 3.75°	64 / 0.01 hPa	REF1	Austin (2002); Struthers et al. (2004)

Table 6-4. Continued.

UMSLIMCAT	University of Leeds, U.K.	M. Chipperfield W. Tian	2.5° × 3.75°	64 / 0.01 hPa	REF1 REF2	Tian and Chipperfield (2005)
WACCM (v.3)	NCAR, U.S.	B. Bovillei R. Garcia A. Gettelman D. Kinnison D. Marsh F. Sassi	4° × 5°	66 / 4.5×10^{-6} hPa	3×REF1[a] 3×REF2 2×NCC	Park et al. (2004); Richter and Garcia (2006)

GFDL, Geophysical Fluid Dynamics Laboratory; NIES, National Institute for Environmental Studies; MSC, Meteorological Service of Canada; DLR, Deutschen Zentrum für Luft- und Raumfahrt; NASA, National Aeronautics and Space Administration; GSFC, Goddard Space Flight Center; IPSL, Institut Pierre Simon Laplace; MPI, Max-Planck-Institut; MRI, Meteorological Research Institute; PMOB/WRC, Physical-Meteorological Observatory/World Radiation Center; ETHZ, Eidgenössische Technische Hochschule Zurich; NIWA, National Institute of Water and Atmospheric Research; NCAR, National Center for Atmospheric Research.

[a] REF1 but with SSTs from the Smith/Reynolds dataset (J. Hurrell, private communication) and without QBO

[b] SCN2 without QBO

[c] REF1 without QBO, solar cycle, and volcanic eruptions

[d] REF1 without QBO and solar cycle

[e] Different SSTs were used in each simulation

features, e.g., very low horizontal resolution (ULAQ) or a low upper boundary (E39C). For the remaining CCMs there is, in general, reasonable agreement with observations. In the upper stratosphere, the model agreement with age of air observations is poorer, with most models underestimating the age (not shown). However, in general the mean age of air and the tape recorder are in better agreement than reported in the Hall et al. (1999) assessment of 2-D and 3-D CTMs.

The ability of CCMs to reproduce past stratospheric chlorine and bromine concentrations clearly affects the confidence that we can place in their projections of future ozone changes, particularly in the Antarctic. Eyring et al. (2006) examined modeled HCl and inorganic Cl_y fields, and again found a large model spread, with some large deviations from observations, see Figure 6-7(c) and Figure 6-8(a). The differences are most pronounced in the polar lower stratosphere, where peak Cl_y varies from around 1 ppb to over 3.5 ppb. Measurements of Cl_y in the Antarctic lower stratosphere (symbols in Figure 6-8(a)) clearly show that peak values of Cl_y close to or less than 2.5 ppb, as simulated by several CCMs, are unrealistic. Transport deficiencies are a major contributor to deficiencies in the simulated HCl and Cl_y, and the models discussed above that did not perform well for transport diagnostics also showed differences from observed HCl. In the MRI model, the age of air decreases significantly with time and, unlike in all other models and observations, Cl_y does not peak around 2000 but continues to increase until after 2015. This unrealistic continued increase of Cl_y lowers the confidence we can place in this simulation. Transport deficiencies do not, however, explain all of the differences. The initial decrease in Cl_y in UMSLIMCAT is due to wrong initial conditions used in this simulation. AMTRAC and UMETRAC have higher HCl and Cl_y than other models but similar CH_4 and mean age of air, and presumably similar transport (Figure 6-7 and 6-8). The additional Cl_y results from photolysis rates of organic chlorine species being artificially increased by 25% in AMTRAC and UMETRAC so that the Cl_y in the upper stratosphere is in close agreement with observed Cl_y. Although this adjustment of the photolysis rates improves the agreement with observed Cl_y in the upper stratosphere and polar lower stratosphere (Figure 6-8(a)), HCl (and also Cl_y) in the extrapolar lower stratosphere is unrealistically large (Figure 6-7(c)). It is not clear whether the 25% increase in the photolysis rates is responsible for the enhanced extrapolar Cl_y.

The CCMs are generally able to reproduce the observed amplitude and phase of the mean annual cycle in total column ozone, except over southern high latitudes (see right panels in Figure 3-26, Chapter 3). However, most models exhibit large offset biases in the mean annual cycle, with the majority overestimating total column ozone. Although it is not possible to trace all differences in the simulated ozone to deficiencies in the simulated temperature and tracers, in some cases a link can be made. For example, the models with low tropical and midlatitude CH_4 have high ozone (MAECHAM4CHEM and

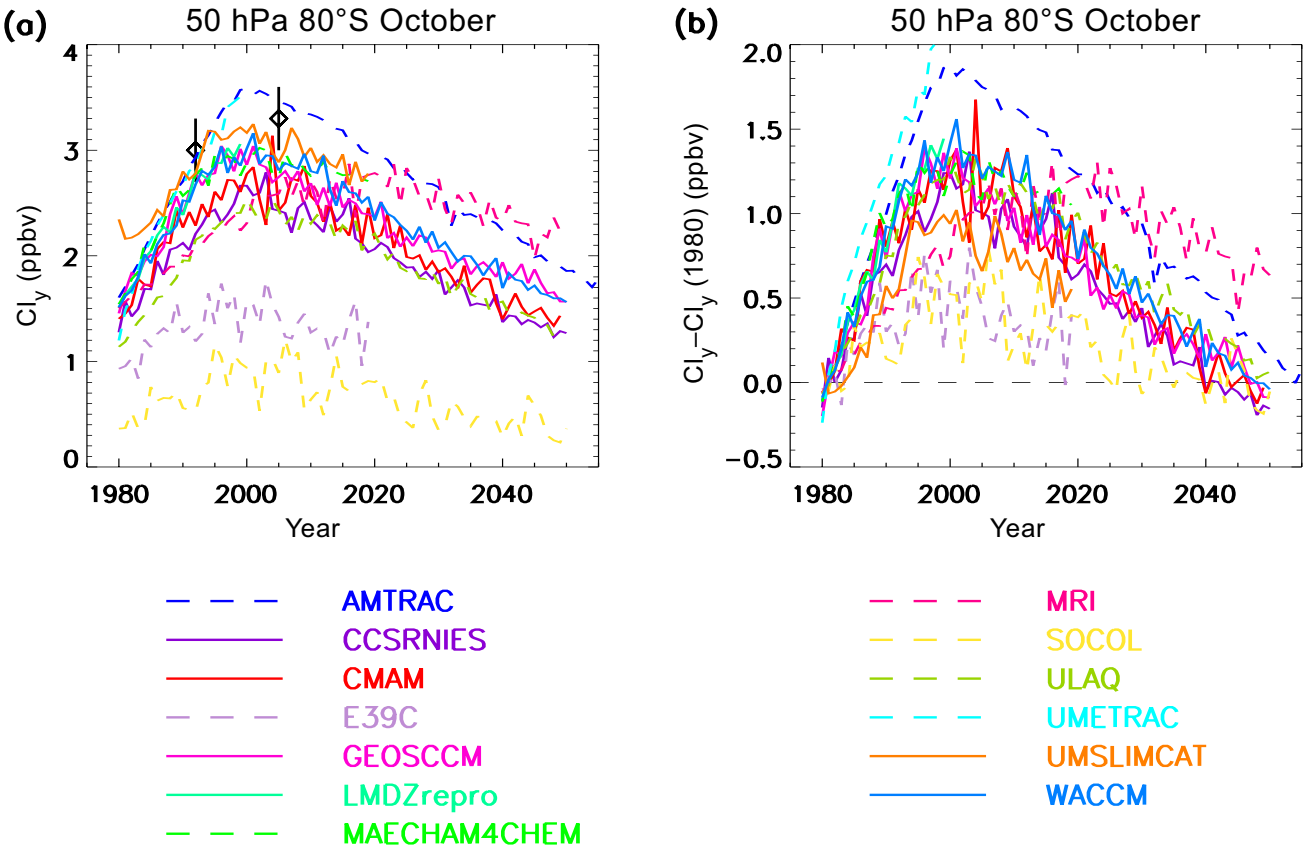

Figure 6-8. October zonal mean values of total inorganic chlorine (Cl$_y$ in ppb) at 50 hPa and 80°S from CCMs. Panel (a) shows Cl$_y$ and panel (b) difference in Cl$_y$ from that in 1980. The symbols in (a) show estimates of Cl$_y$ in the Antarctic lower stratosphere in spring from measurements from the UARS satellite in 1992 and the Aura satellite in 2005, yielding values around 3 ppb (Douglass et al., 1995; Santee et al., 1996) and around 3.3 ppb (see Figure 4-8), respectively.

MRI), those with low Cl$_y$ in polar regions have smaller ozone reductions there (SOCOL and E39C), and the model with the largest cold bias in the Antarctic lower stratosphere in spring (LMDZrepro) simulates very low ozone.

CCMs show a large range of ozone trends over the past 25 years (see left panels in Figure 3-26 of Chapter 3) and large differences from observations. Some of these differences may in part be related to differences in the simulated Cl$_y$, e.g., E39C and SOCOL show a trend smaller than observed, whereas AMTRAC and UMETRAC show a trend larger than observed in extrapolar area weighted mean column ozone. However, other factors also contribute, e.g., biases in tropospheric ozone (Austin and Wilson, 2006).

The CCM evaluation discussed above and in Eyring et al. (2006) has guided the level of confidence we place on each model simulation. The CCMs vary in their skill in representing different processes and characteristics of the atmosphere. Because the focus here is on ozone recovery due to declining ODSs, we place importance on the models' ability to correctly simulate stratospheric Cl$_y$ as well as the representation of transport characteristics and polar temperatures. Therefore, more credence is given to those models that realistically simulate these processes. Figure 6-7 shows a subset of the diagnostics used to evaluate these processes and CCMs shown with solid curves in Figures 6-7, 6-8, 6-10 and 6-12 to 6-14 are those that are in good agreement with the observations in Figure 6-7. However, these line styles should not be over-interpreted as both the ability of the CCMs to represent these processes as well as the relative importance of Cl$_y$, temperature, and transport vary between different regions and altitudes. Also, analyses of model dynamics in the Arctic, and differences in the chlorine budget/partitioning in these models, when available, might change this evaluation for some regions and altitudes.

6.6.3 Midlatitude and Tropical Ozone

Figures 6-9 and 6-10 show the time evolution through the 21st century of annual means of monthly total column ozone anomalies from the 2-D models and CCMs, respectively, for four different regions: extrapolar (60°S to 60°N), tropics (25°S to 25°N), northern midlatitudes (35° to 60°N), and southern midlatitudes (35° to 60°S). For the 2-D models, ozone from the P1 and F1 simulations is shown, while for the CCMs the ozone is from REF1 and REF2 or SCN2 (depending on the CCM) simulations (see Table 6-4 for description of simulations). Multiple curves are shown for CCMs that ran multiple simulations with the same forcing. The method used to calculate the ozone anomalies is detailed in Eyring et al. (2006).

The evolution of the ozone anomalies is qualitatively similar for both the 2-D models and the CCMs: the lowest ozone occurs around 2000 within a broad minimum after which ozone increases, as expected from decreasing EESC beyond 2000. A clear difference between the 2-D model and CCM projections is the year-to-year fluctuations in the ozone anomalies. The 2-D models show a smooth ozone evolution, whereas the CCMs show large interannual variability. The variability in the CCMs arises from internal dynamics and variations in prescribed sea surface temperatures with time. Variability associated with the QBO and 11-year solar cycle is also included in some CCM simulations (see Table 6-4) and contributes to the interannual and longer time variations. Since the focus is on decadal changes, the ozone anomalies plotted in Figure 6-10 have been smoothed using a 1:2:1 filter applied 5 times iteratively. There is a large spread in projected ozone anomalies during the beginning of the 21st century (2000 to 2020). Two CCMs (AMTRAC and MRI) show much larger ozone anomalies than the other models. These two models also have much larger HCl and Cl_y during this period (AMTRAC because of increased CFC photolysis rates, and MRI because of slower circulation; see discussion in Section 6.6.2), which may explain part of the larger ozone anomalies.

Averaged between 60°N and 60°S, total column ozone is projected to increase between 2000 and 2020 in all models except MRI (see above discussion), with most of the increase of 1% to 2.5% occurring after 2010. Over midlatitudes, the majority of the models predict an increase of 1.5% to 3.5%, while over the tropics smaller ozone increases of less than 2% are projected. The evaluation of the timing of ozone minima is biased by the large response to Mt. Pinatubo in the 2-D models, and obscured by interannual variability in the CCMs. If smoothed CCM anomalies are used (as shown in Figure 6-10) and, to avoid local ozone minima caused by Mt. Pinatubo, only minima after 1996 are considered, both classes of model predict that minimum ozone values have already occurred between 60°S and 60°N. In midlatitudes, 2-D models predict ozone minima between 1997 and 2001 while the CCMs (again with the exception of MRI) predict ozone minima between 1997 and 2007 with no clear hemispheric differences. Because the exact timing of minimum ozone in some of the CCM simulations might be affected by the solar cycle (e.g., Dameris et al., 2006) or other factors, the ozone minima detected in the CCMs are not synonymous with ozone turnaround and should not be interpreted as stage (ii) of ozone recovery.

It is expected that EESC in the midlatitude lower stratosphere will decrease to its 1980 value between 2040 and 2050 (see box 8-1). If no other factors played a role, it would be expected that ozone would increase to its 1980 values at the same time. However, if there are changes in temperature, transport, or the abundance of other gases, ozone may return to 1980 values earlier or later than EESC. Figure 6-9 shows that total column ozone in the interactive 2-D models that include temperature feedbacks from changes in WMGHGs (GSFC-INT, LeedsBremen, NOCAR) is above 1980 values between 2040 and 2050. Ozone averaged between 60°S and 60°N in these models returns to 1980 values between 2025 and 2035, so that by the time EESC returns to 1980 values, ozone is 0.5% to 3.0% above 1980 values. In the tropics and northern midlatitudes, ozone returns to 1980 values between 2020 and 2030, while over southern midlatitudes this happens somewhat later, between 2025 and 2040. The increase in ozone to levels higher than would be expected from ODS concentrations alone results from stratospheric cooling due to increased concentrations of WMGHGs. In contrast to the interactive 2-D models, the non-interactive 2-D models predict that column ozone will be less than or around 1980 values in 2040, and averaged between 60°S and 60°N, column ozone returns to 1980 values about 5 years (but up to 15 years) later than in the interactive models. This is consistent with temperature changes playing a major role in the increases in ozone.

The CCM simulations that extend to 2050 show a similar recovery process over midlatitudes as the interactive 2-D models. Most CCMs (all but one/two in northern/southern midlatitudes) predict midlatitude ozone to be on average higher than 1980 values between 2040 and 2050, with increases to 1980 values generally occurring between 2005 and 2035 over northern midlatitudes and over southern midlatitudes somewhat later between 2025 and 2040, in agreement with the interactive 2-D models (Figure 6-10). The earlier return of northern midlatitude ozone to pre-1980 values is echoed in the hemispheric differences in ozone anomalies between 2040 and

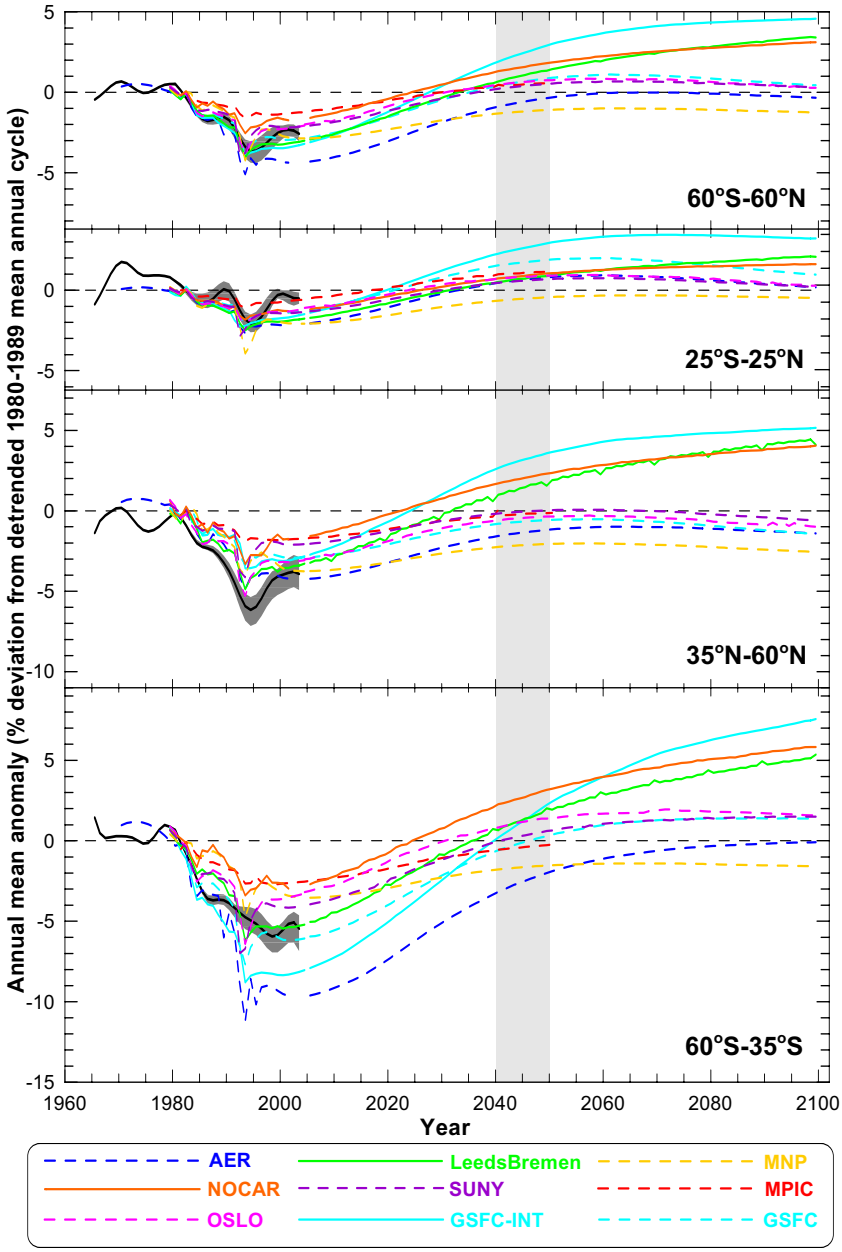

Figure 6-9. Annual mean zonal mean total column ozone anomalies from the P1 (1980-2004) and F1 (2005-2100) runs (Appendix 6A) from all of the 2-D models (colored lines; solid for interactive models and dashed for non-interactive models) and from four observational datasets (thick black line and gray shaded area show the mean and range of observed anomalies; see Chapter 3). Area-weighted zonal mean time series are shown for the global region (60°S to 60°N), the equatorial region (25°S to 25°N), the northern midlatitude region (35°N to 60°N), and the southern midlatitude region (60°S to 35°S) to match the analysis regions used in Chapter 3. The observational time series have been smoothed by applying a 1:2:1 filter iteratively five times. The filter width is reduced to 1 at the ends of the time series, effectively reproducing the original data and avoiding anomalous edge effects. The light gray shading between 2040 and 2050 shows the period when EESC is expected to return to 1980 values. Monthly anomalies were calculated by subtracting a detrended mean annual cycle, calculated over the period 1980-1989, from each time series. The annual cycle was detrended by fitting a regression model with seasonally dependent trends to the data and then reconstructing the "1980" mean annual cycle using the stationary components of the regression model. For further details on the method for calculating the anomalies, see Eyring et al. (2006).

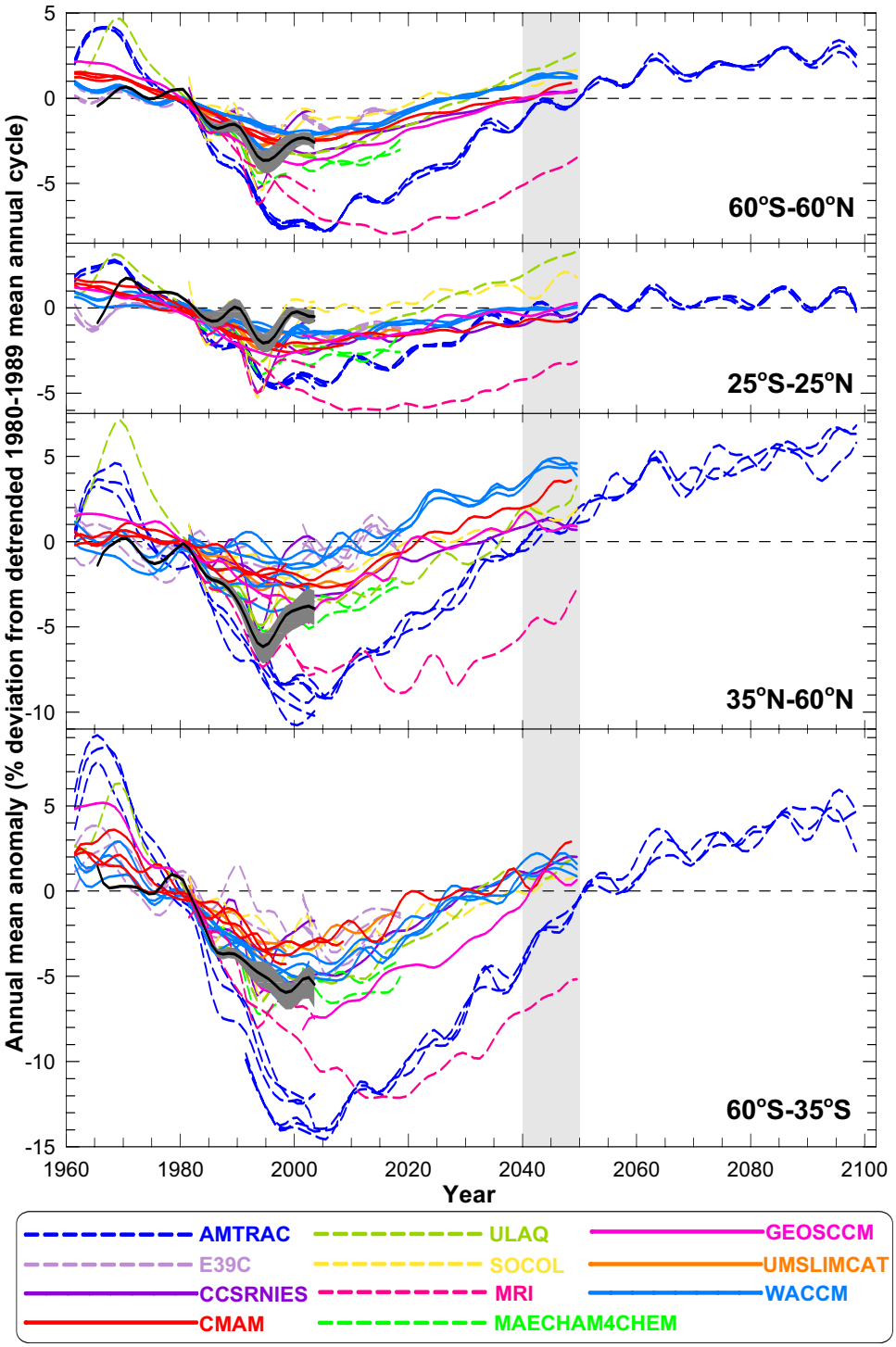

Figure 6-10. Annual mean zonal mean total column ozone anomalies from CCMs (colored lines) and from four observational datasets (thick black line and gray shaded area show the mean and range of observed anomalies; see Chapter 3). The time series are formed using the REF1 and REF2 or SCN2 simulations of each model (see Table 6-4). The time series have been smoothed as in Figure 6-9. The light gray shading between 2040 and 2050 shows the period when EESC is expected to return to 1980 values. As for the 2-D model results, the anomalies were calculated by subtracting the detrended 1980-1989 mean annual cycle. The mean annual cycles subtracted from the raw monthly means to calculate these anomalies are shown in Figure 3-26. For further details on the method for calculating the anomalies, see Eyring et al. (2006).

2050 (NH value of 0.5 to 5%; SH value of −0.5 to 3%). The two exceptions to the above are AMTRAC and MRI, which show a slower return of ozone to 1980 values such that ozone is below 1980 values in 2040. The later return of ozone to pre-1980 values in AMTRAC and MRI is consistent with the later decrease of Cl_y to 1980 values in these models (although other factors, such as biases in the troposphere (Austin and Wilson, 2006), may also contribute).

The recovery process of tropical ozone differs between the CCMs and interactive 2-D models. As discussed above, the interactive 2-D models predict tropical ozone to be above pre-1980 levels by 2040. In contrast, the majority of the CCMs predict ozone around or less than 1980 values in 2040. The cause of this difference is not known. Austin and Wilson (2006) noted that during northern spring, tropical ozone remained below 1980 levels out to 2100 in a narrow band around the equator. Rosenfield and Schoeberl (2005), using the GSFC-INT interactive 2-D model, showed that ozone at 51 hPa and 5°N remains low out to 2050 in their model as a result of increasing CO_2, which cools the upper stratosphere, slows ozone gas-phase destruction reactions, and increases ozone there, which in turn reduces the penetration of UV to the lower stratosphere, which reduces ozone production there (a reverse of the "self-healing" effect). However, given that the GSFC-INT model also shows ozone exceeding pre-1980 levels between 25°S and 25°N (Figure 6-9), these suppressed ozone concentrations in the tropical lower stratosphere must not dominate column ozone changes.

After 2050, the ozone changes primarily reflect changes in WMGHGs. In the non-interactive 2-D models, the ozone is roughly constant or declines. In contrast, in the interactive 2-D models and in the one CCM that ran beyond 2050 (Austin and Wilson, 2006), ozone continues to slowly increase (except tropical ozone in AMTRAC and in the GSFC-INT model). By the end of the 21st century, these models predict that ozone averaged between 60°S and 60°N will be 2% to 5% above 1980 values.

In the simulations presented above, only a single scenario for WMGHG emissions has been considered. However, the sensitivity to temperatures and/or composition caused by WMGHG increases has been examined in other simulations. For example, Rosenfield et al. (2002) used an interactive 2-D model to examine the impact of CO_2 increase-induced cooling on ozone recovery and found that ozone returns to 1980 values 10 to 20 years earlier in many latitudes and seasons. Randeniya et al. (2002) used a non-interactive 2-D model to examine the impact of WMGHG-induced atmospheric composition changes on ozone through the 21st century and showed that in northern midlatitudes, the ozone recovery depended greatly on the emissions scenarios used to drive the model. After 2050, NO_x increases due to N_2O increases caused stratospheric ozone levels to start to fall, and this loss was exacerbated if future methane levels remained approximately constant, rather than growing, as assumed in many scenarios.

The combined impact of CO_2-induced cooling and changes in N_2O was subsequently examined by Chipperfield and Feng (2003), using the Leeds-Bremen interactive 2-D model. They performed two simulations, one with and the other without temperature changes due to increasing CO_2, for three different WMGHG scenarios (one with high emissions (A1FI), one with low emissions (B1), and a third with A1FI emissions except with reduced CH_4 emissions). As shown in Figure 6-11, these calculations indicate that the inclusion of the CO_2-induced cooling overcomes the N_2O chemical effect and leads to ozone reaching 1980 levels or above between 2030 and 2050, depending on the WMGHG scenario used. Similar results were obtained in NOCAR simulations performed for this Assessment (not shown). Consistent with Randeniya et al. (2002), Figure 6-11 also shows that for the cases where the CO_2-induced cooling is excluded, ozone does not return to pre-1980 values in the 21st century. Therefore, the CO_2-induced cooling and the N_2O chemical effect oppose each other, with the net effect dependent on the WMGHG scenario chosen.

The sensitivity of ozone recovery to WMGHG scenarios has also been examined using CCMs that include a more complete representation of climate-ozone feedbacks (e.g., the variability in tropospheric wave forcing due to climate change). As discussed in Chapter 5, simulations were also repeated for several CCMs with fixed WMGHGs, rather than increasing WMGHGs as in the "A1B" scenario. These simulations show higher stratospheric temperatures and slower increases in midlatitude ozone than in the simulations with increasing WMGHGs (see Figure 5-25 of Chapter 5).

6.6.4 Polar Ozone

As discussed in Chapter 5, the processes affecting ozone recovery in the polar regions are different from those influencing extrapolar recovery. For example, WMGHG-induced cooling of the stratosphere reduces ozone destruction in extrapolar regions, but enhances it in the polar lower stratosphere where heterogeneous chemistry dominates. To investigate the evolution of polar ozone through the 21st century, we focus on the CCMs as 2-D models do not include the three-dimensional processes that play a key role in polar ozone depletion and recovery. Several dif-

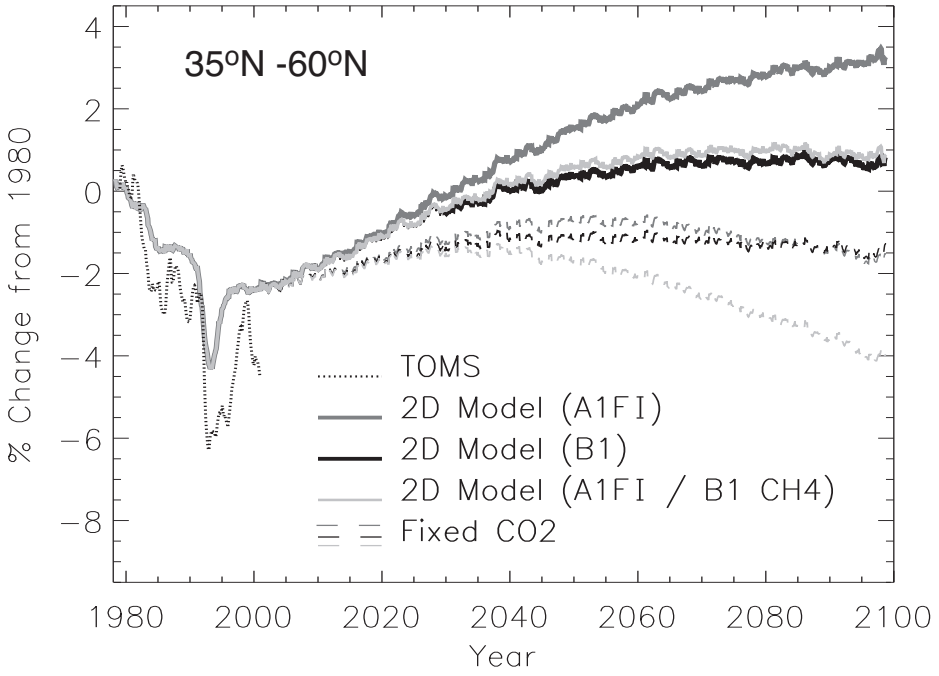

Figure 6-11. Variation in Northern Hemisphere midlatitude total column ozone (% change since 1980) from six runs of a 2-D model. The simulations used three different WMGHG scenarios (A1FI, B1, and A1FI with B1 CH_4 emissions), with results shown with (solid lines) and without (dashed lines) stratospheric cooling due to CO_2 increases. Also shown are observed past changes from satellite data. From Chipperfield and Feng (2003).

ferent diagnostics of polar ozone from the CCMs are considered, including:

- springtime total column ozone anomalies for the Arctic (March, 60°N-90°N) and Antarctic (October, 60°S-90°S), Figure 6-12;
- the minimum total column ozone poleward of 60°N for March-April (Arctic) and 60°S for September-October (Antarctic), Figure 6-13;
- the ozone mass deficit (Bodeker et al., 2005) from September to October, Figure 6-14; and
- the maximum Antarctic ozone hole area between September and October, Figure 6-14.

A discussion of the Antarctic ozone hole indices is provided in Chapter 4.

We examine these diagnostics for the same time periods as above: the beginning of the century (2000-2020) when EESC declines substantially, mid-century (2060-2070) when EESC is expected to decrease to 1980 values, and the end of the century (2090-2100) when ODSs are not expected to play a role in controlling polar ozone.

6.6.4.1 The Antarctic

In the Antarctic, the general characteristics of the ozone recovery are similar in all models and similar to the CCM projections shown in Austin et al. (2003) and WMO (2003), namely, the peak depletion occurs around 2000 within a broad minimum, followed by a slow increase in ozone values. All CCMs show Antarctic ozone increasing between 2000 and 2020, although the evolution varies between models and between diagnostics. In general, column ozone increases by around 5% to 10% during this period. In nearly all models, the year of lowest October column ozone anomalies occurs between 1997 and 2010 but, as shown in Figures 6-12, 6-13, and 6-14, the response of the ozone diagnostic to changes in ODSs varies between the diagnostics. The increase in 60°-90°S October ozone anomalies and minimum Antarctic ozone is relatively slow, with values remaining constant between 2000 and 2010 in many models, whereas there is a relatively fast decrease in the ozone mass deficit. This behavior matches the differences in response between different Antarctic ozone hole indices seen in observations (Bodeker et al., 2005). The fact that some of the CCMs suggest that minimum October ozone anomalies have already occurred in the Antarctic may appear to contradict the conclusion made in Section 6.5.3 that neither the first, nor second stage of Antarctic ozone recovery has been detected in observations. It should be noted that the availability of model results beyond 2005, as opposed to measurements that terminate in 2005, facilitates the detection of the minimum. Ozone turnaround in measurements may have already occurred but lack of data beyond 2005 precludes its statistical detection. Nevertheless, because the turnaround in ozone as simulated in the CCMs has not been attributed here to changes in EESC, this behavior cannot be interpreted as stage (ii) of ozone recovery.

There is a wide range in the simulated peak ozone depletion in the CCMs. For example, the smoothed wintertime minimum Antarctic ozone values in the CCMs vary

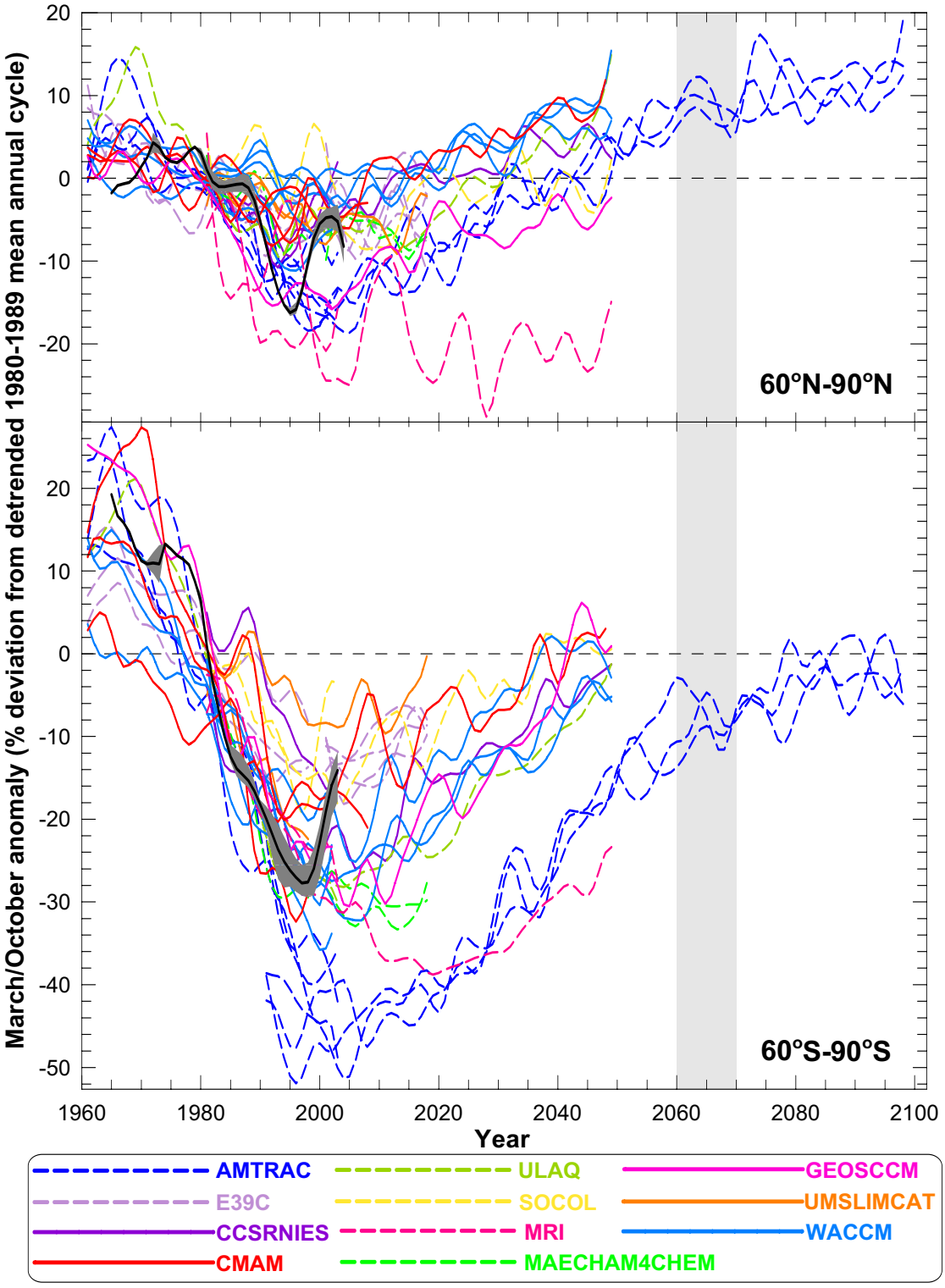

Figure 6-12. Upper panel: March Arctic (60°N to 90°N) total column ozone anomalies from CCMs (colored lines) and from 4 observational datasets (thick black line and gray shaded area show the mean and range of observed anomalies; see Chapter 3). Lower panel: as for the upper panel but October Antarctic (60°S to 90°S) total column ozone anomalies. Model simulations are as in Figure 6-10. The time series have been smoothed as in Figure 6-10. The light gray shading between 2060 and 2070 shows the period when EESC is expected to return to 1980 values.

between around 60 DU and 120 DU compared with observed values around 80 DU (Figure 6-13(b)), while the peak smoothed ozone mass deficit varies between 5 and 33 million tons compared with observed values around 31 million tons (Figure 6-14(a)). These variations highlight the deficiencies in some of the CCM simulations of the present-day ozone hole. Note, however, that because both the ozone hole area and the ozone mass deficit are based on 220 DU thresholds, a general high bias in the global-mean total ozone fields will generate a bias in these two diagnostics (e.g., most pronounced in MAECHAM-4CHEM).

There is a wide spread in the projected Antarctic ozone anomalies in 2050 and in the projected date when Antarctic ozone increases to or around 1980 values. The anomalies in 60°-90°S ozone in 2050 (see Figure 6-12) vary from around –24% to 3%, while the date for Antarctic ozone to increase to 1980 values varies between 2035 and 2095. However, this wide spread is mainly due to a few models (AMTRAC, MRI; see further discussion); in the majority of the CCMs, ozone is around 1980 values between 2040 and 2050.

There is no simple relationship in the CCMs between the date that Antarctic ozone increases to 1980 values and either the date of the minimum in Antarctic ozone or the ozone anomaly at this date. Hence, comparison of the simulated ozone hole with observations (as shown in Figures 6-13 and 6-14) does not provide a good indicator of differences in the CCM projections of the future ozone hole, and the wide spread shown in Figures 6-12 to 6-14.

However, some insight into the model differences can be obtained from comparisons of inorganic chlorine (Cl_y) in the models. A relationship is expected between the decrease in Cl_y and increase in ozone, and, in general, the increase in Antarctic ozone follows the decrease in Cl_y in the CCMs. As shown in Figure 6-8, there is a large spread in the simulated Antarctic Cl_y, including in the peak value and the date at which the Cl_y decreases to 1980 values. Models with a smaller peak have an earlier return of Cl_y to pre-1980 levels (e.g., SOCOL and E39C) and those with a larger peak have a later return (e.g., AMTRAC). Comparison with observations showed that peak Cl_y in several models is unrealistically low (see Section 6.6.2), and the above analysis indicates that the return to pre-1980 values of both Cl_y and ozone will be too early in these models. We thus put more weight on results from CCMs with higher, and more realistic, Cl_y. These models predict Cl_y and ozone back to pre-1980 values around or later than 2050. The MRI model simulates a later return of ozone to pre-1980 values due to an unrealistic too slow decrease of Cl_y after 2000 and we put less weight on this model simulation. The Cl_y in AMTRAC matches the observations best, and predicts the latest return to pre-1980 values (Figure 6-8). The better agreement of polar Cl_y with observations gives support for this late return, but the justification for altering CFC photolysis rates has to be questioned (see Section 6.6.2).

The late return to pre-1980 values in the AMTRAC model is, nevertheless, consistent with the parametric modeling study of Newman et al. (2006). Using a parametric model of spring Antarctic ozone amounts that includes EESC levels over Antarctica (see Box 8.1 of Chapter 8) and analyzed Antarctic stratospheric temperatures, they predicted that the ozone hole area will remain constant until around 2010, that a decrease of the ozone hole area would not be statistically detectable until around 2024, and that return to pre-1980 levels in the Antarctic would not occur until around 2068; see Figure 6-14(b).

AMTRAC is the only CCM to run past 2050. This model predicts that springtime Antarctic ozone will be close to or just below (–7% to 3%) 1980 values by the end of the century (2090-2100). However, uncertainties in the projection are high because they are based on a single model and single WMGHG concentration scenario.

6.6.4.2 The Arctic

As in the other regions, Arctic ozone is projected to increase from 2000 to 2020 (see Figures 6-12 and 6-13). The increases range between 0% and 10% and there is large interannual variability. Using the smoothed minimum Arctic ozone or 60°-90°N ozone anomalies, where the smoothing reduces the large variability, the date of minimum ozone occurs between 1997 and 2015 in nearly all of the models. This time range is similar to that for the Antarctic. As in the Antarctic, although the timing of the minimum anomaly is similar between models, there is a substantial variation in the magnitude of the ozone when this occurs, with the smoothed minimum Arctic ozone varying from around 200 DU to over 300 DU, compared with around 220 DU in the observations. This again highlights some substantial biases in many of the models.

Most CCMs that have been run to 2050 show Arctic ozone values larger than 1980 values in 2050. In other words, all CCMs show Arctic ozone increasing to pre-1980 values before 2050 (and before EESC returns to 1980 concentrations; 2060-2070). There is a wide range of dates for Arctic ozone to increase to 1980 values, with the date that smoothed minimum Arctic ozone increases to 1980 values varying between around 2010 and 2040. Although there are large differences in the CCM simulations of Arctic ozone, all, except MRI, show an increase to pre-

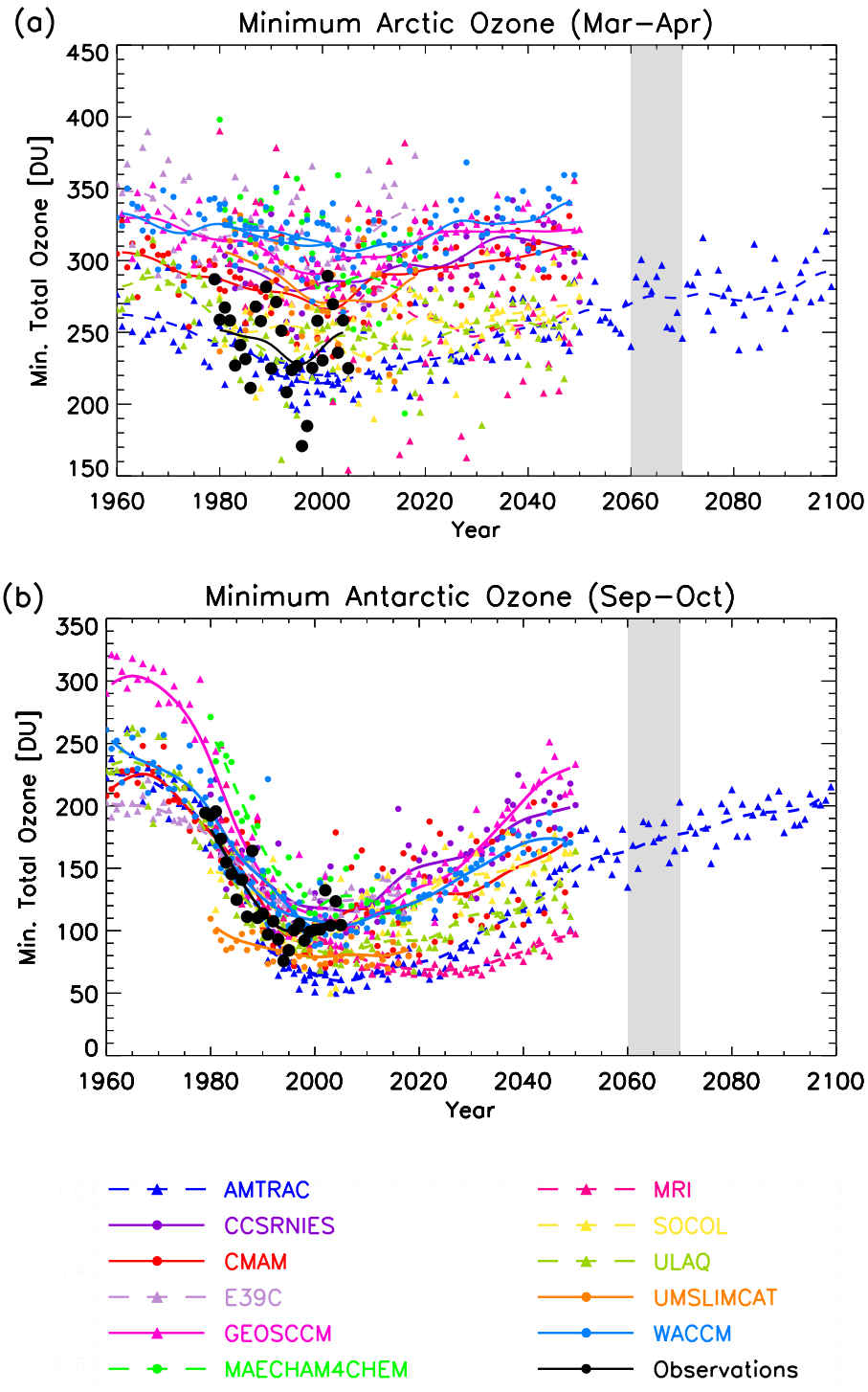

Figure 6-13. (a) Minimum Arctic total column ozone for March to April and (b) minimum Antarctic total column ozone for September to October for various transient CCM simulations. Model simulations are as in Figure 6-10, except a single ensemble simulation is shown for each model. Model results are compared with observations calculated using the National Institute of Water and Atmospheric Research (NIWA) combined total column ozone database (Bodeker et al., 2005). Solid and dashed curves show smoothed data derived by applying a 1:2:1 filter iteratively 30 times. The filter width is reduced to 1 at the ends of the time series, effectively reproducing the original data and avoiding anomalous edge effects. The light gray shading between 2060 and 2070 shows the period when EESC is expected to return to 1980 values.

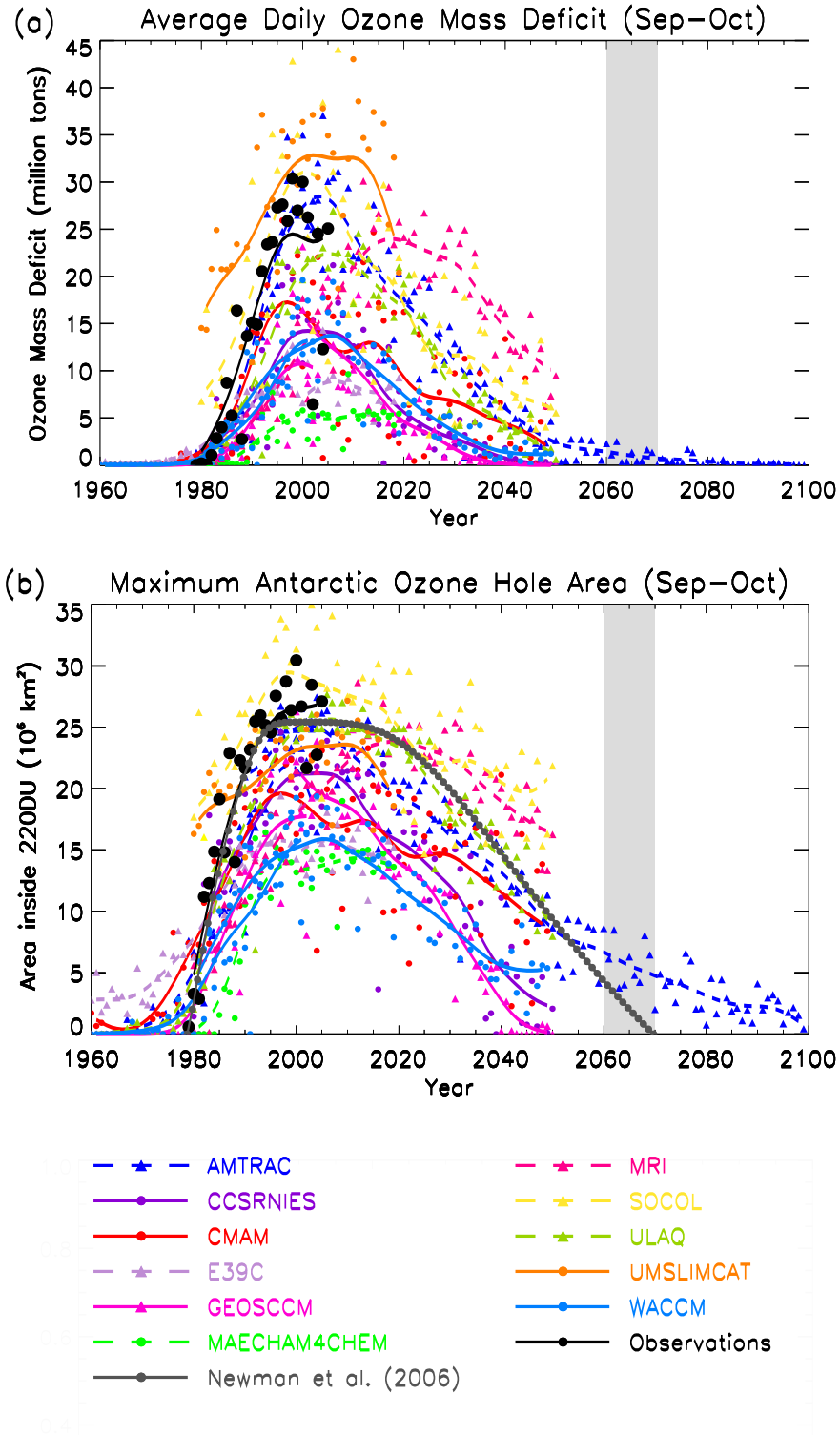

Figure 6-14. (a) The Antarctic September to October average daily ozone mass deficit for each year from each CCM and (b) the maximum Antarctic ozone hole area between September and October. Model simulations are as in Figure 6-10, except a single ensemble simulation is shown for each model. Model results are compared with observations calculated using the National Institute of Water and Atmospheric Research (NIWA) combined total column ozone database (Bodeker et al., 2005). The curves show the data smoothed as in Figure 6-13. Gray circles show the projection from Newman et al. (2006). The light gray shading between 2060 and 2070 shows the period when EESC is expected to return to 1980 values.

1980 ozone before or around 2050 with no indication of severe Arctic ozone loss over this time.

In all CCMs that have been run long enough, Arctic ozone increases to 1980 values before Antarctic ozone does. In some models the difference is only a few years, but in others the difference is over 25 years. The projected evolution of Arctic ozone does not follow the evolution of halogens as closely as in the Antarctic, i.e., the spread of the projected Arctic ozone is not strongly related to the spread in simulated Cl_y (the simulated Arctic Cl_y is similar to that shown in Figure 6-8). This indicates that changes in other factors (e.g., temperature and transport) play a significant role in determining when Arctic ozone returns to pre-1980 values. Austin and Wilson (2006) reported that the earlier return to pre-1980 values in the Arctic in AMTRAC results from both an increased Brewer-Dobson circulation and reduced gas-phase ozone depletion in a cooler stratosphere. However, it is unclear whether this is occurring in all models. For example, in the E39C, ULAQ, and WACCM simulations with fixed WMGHGs discussed in Chapter 5, the return to pre-1980 values is very similar to that in simulations with increasing WMGHGs presented here (see Figure 5-26 of Chapter 5). This suggests that in these models, there is little impact of increased WMGHGs on Arctic ozone recovery before 2050.

Projections from AMTRAC, the only CCM to run past 2050, suggest that Arctic ozone in 2090 to 2100 will be substantially above (8% to 19%) 1980 values. This is in contrast to Antarctic ozone in this model, which is close to or just below 1980 values by the end of the century.

The increase in the Arctic column ozone minima in the above CCM simulations is much faster than the empirical estimation of Knudsen et al. (2004), where the Arctic ozone losses would increase until 2010-2015 and decrease only slightly afterwards. However there are large uncertainties in the Knudsen et al. calculations: the observed temperature and water vapor trends used in the analysis are uncertain, and most important, it is unlikely that the past trends will (as they assumed) continue unchanged into the future (see Austin, 2004; Pitari, 2004). Given the likelihood of changes in trends in the Arctic, we put more weight on the CCM projections, which attempt to capture these changes, than the Knudsen empirical predictions.

6.6.5 Uncertainties in Model Projections and Open Questions

Sources of uncertainty in model projections of future ozone range from those intrinsic to the models, such as uncertainties in parameterizations and adequate incorporation of feedbacks, to those external, such as uncertainties in the emissions scenarios and sea surface temperature datasets used to drive the models. Many of the intrinsic sources of uncertainties in CCMs are discussed in Chapter 5 and the uncertainties resulting from projections of future ODS emissions are discussed in Chapter 8. The purpose of this section is to discuss some of the processes that are not included in the models that may contribute to uncertainty in ozone projections.

The model results presented above have focused on one WMGHG emissions scenario (see Appendix 6A). The IPCC Special Report on Emissions Scenarios (SRES) (IPCC, 2000) A1B scenario is by no means the most likely scenario, and the use of different, but possibly equally likely, scenarios is expected to cause different projections of future ozone, see Figure 6-11. Furthermore, the SRES scenarios define only changes in anthropogenic emissions and not concurrent changes in natural emissions due, for example, to changes in surface climate. Climate change-induced increases in emissions of halogenated very short-lived sources gases, changes to their transport to the tropical tropopause layer (TTL), and their degradation to bromine, chlorine, and iodine (see Section 2.4 of Chapter 2) have the potential to change tropical ozone abundances in the future. Given the current resolution of the TTL region in CCMs, we cannot fully assess this question. Currently our understanding from transport studies would indicate that only a small fraction of air is directly lifted vertically through the TTL into the lower tropical stratosphere, but there are indications that the "sideways" transport into the extratropical stratosphere might be significant and sometimes fast (Levine et al., 2006).

At present, the prescribed model boundary conditions are not the emissions scenarios themselves but concentration scenarios derived from the emissions scenarios (Prather and Ehhalt et al., 2001). This decoupling of the processes linking changes in emissions to changes in concentrations of WMGHGs and ODSs neglects feedbacks that could be important, e.g., future increases in stratospheric ozone may change tropospheric photolysis rates through enhanced absorption of solar UV, and change tropospheric ozone levels by increasing the stratosphere-troposphere exchange source of ozone (Hauglustaine et al., 2005). These in turn affect tropospheric oxidizing capacity, which affects WMGHG and ODS lifetimes. The effects of such changes on lifetimes have been ignored in the construction of ODS and WMGHG concentration scenarios; see Section 8.3.1 of Chapter 8 and Prather and Ehhalt et al. (2001), respectively. Natural processes, such as volcanic eruptions (see Section 6.3.6), could also affect tropospheric oxidizing capacity and/or change the effectiveness of stratospheric ODSs in depleting ozone.

New anthropogenic source gases, currently excluded from emissions scenarios, may become impor-

tant in the future, e.g., fugitive emissions of hydrogen from a hydrogen economy. Tromp et al. (2003) estimated that a hydrogen economy could cause stratospheric water vapor increases of up to 35% and decrease ozone by up to 10% in polar regions during spring. However, Warwick et al. (2004) found a much reduced effect on stratospheric ozone on the order of 0.5% or less. This reduced estimate is the result of an assumed smaller leakage rate of hydrogen combined with the inclusion of reduced CO, NO_x, CH_4, and nonmethane hydrocarbons due to the reduction of fossil fuel usage. Furthermore, the timing of the conversion to a hydrogen economy with respect to the reduction of halogen loading is a major factor, because the coupling to chlorine chemistry causes most of the ozone loss. If the shift to a hydrogen economy occurs primarily after 2020 (Kammen and Lipman, 2003), the potential harm due to the increase in anthropogenic hydrogen emission can be prevented.

REFERENCES

Akiyoshi, H., T. Sugita, H. Kanzawa, and N. Kawamoto, Ozone perturbations in the Arctic summer lower stratosphere as a reflection of NO_x chemistry and planetary scale wave activity, *J. Geophys. Res.*, *109*, D03304, doi: 10.1029/2003JD003632, 2004.

Andersen, S.B., E.C. Weatherhead, A. Stevermer, J. Austin, C. Brühl, E.L. Fleming, J. de Grandpré, V. Grewe, I. Isaksen, G. Pitari, R.W. Portmann, B. Rognerud, J.E. Rosenfield, S. Smyshlyaev, T. Nagashima, G.J.M. Velders, D.K. Weisenstein, and J. Xia, Comparison of recent modeled and observed trends in total column ozone, *J. Geophys. Res.*, *111*, D02303, doi: 10.1029/2005JD006091, 2006.

Andrews, A.E., K.A. Boering, B.C. Daube, S.C. Wofsy, M. Loewenstein, H. Jost, J.R. Podolske, C.R. Webster, R.L. Herman, D.C. Scott, G.J. Flesch, E.J. Moyer, J.W. Elkins, G.S. Dutton, D.F. Hurst, F.L. Moore, E.A. Ray, P.A. Romashkin, and S.E. Strahan, Mean ages of stratospheric air derived from in situ observations of CO_2, CH_4, and N_2O, *J. Geophys. Res.*, *106* (D23), 32295-32314, doi: 10.1029/2001JD000465, 2001.

Austin, J., A three-dimensional coupled chemistry-climate model simulation of past stratospheric trends, *J. Atmos. Sci.*, *59* (2), 218-232, 2002.

Austin, J., Is there really an alternative to the use of coupled chemistry-climate models? Part 1, Interactive comment on "Extrapolating future Arctic ozone losses" by B.M. Knudsen et al., *Atmos. Chem. Phys. Discuss.*, *4*, S1068-S1072, 2004.

Austin, J., and R.J. Wilson, Ensemble simulations of the decline and recovery of stratospheric ozone, *J. Geophys. Res., 111* (D16314), doi: 10.1029/2005JD006907, 2006.

Austin, J., D. Shindell, S.R. Beagley, C. Brühl, M. Dameris, E. Manzini, T. Nagashima, P. Newman, S. Pawson, G. Pitari, E. Rozanov, C. Schnadt, and T.G. Shepherd, Uncertainties and assessments of chemistry-climate models of the stratosphere, *Atmos. Chem. Phys.*, *3*, 1-27, 2003.

Austin, J., J. Wilson, F. Li, and H. Vömel, Evolution of water vapor and age of air in coupled chemistry climate model simulations of the stratosphere, *J. Atmos. Sci.*, in press, 2006.

Beagley, S.R., J. de Grandpré, J.N. Koshyk, N.A. McFarlane, and T.G. Shepherd, Radiative-dynamical climatology of the first-generation Canadian Middle Atmosphere Model, *Atmos. Ocean*, *35* (3), 293-331, 1997.

Bloom, S., A. da Silva, D. Dee, M. Bosilovich, J.-D. Chern, S. Pawson, S. Schubert, M. Sienkiewicz, I. Stajner, W.-W. Tan, and M.-L. Wu, *Documentation and Validation of the Goddard Earth Observing System (GEOS) Data Assimilation System*, *Version 4*, *NASA/TM-2005-104606*, *26*, 187 pp., NASA Goddard Space Flight Center, Greenbelt, Md., 2005.

Bodeker, G.E., H. Shiona, and H. Eskes, Indicators of Antarctic ozone depletion, *Atmos. Chem. Phys.*, *5*, 2603-2615, 2005.

Brasseur, G., and C. Granier, Mount Pinatubo aerosols, chlorofluorocarbons, and ozone depletion, *Science*, *257* (5074), 1239-1242, 1992.

Brönnimann, S., J. Luterbacher, J. Staehelin, T.M. Svendby, G. Hansen, and T. Svenøe, Extreme climate of the global troposphere and stratosphere in 1940-42 related to El Niño, *Nature*, *431* (7011), 971-974, 2004.

Butchart, N., and A.A. Scaife, Removal of chlorofluorocarbons by increased mass exchange between the stratosphere and troposphere in a changing climate, *Nature*, *410* (6830), 799-802, 2001.

Butchart, N., A.A. Scaife, M. Bourqui, J. de Grandpré, S.H.E. Hare, J. Kettleborough, U. Langematz, E. Manzini, F. Sassi, K. Shibata, D. Shindell, and M. Sigmond, Simulations of anthropogenic change in the strength of the Brewer-Dobson circulation, *Clim. Dyn., 27* (7-8), 727-741, 2006.

Chipperfield, M.P., and W. Feng, Comment on: "Stratospheric Ozone Depletion at northern mid-latitudes in the 21st century: The importance of future concentrations of greenhouse gases nitrous oxide and methane," *Geophys. Res. Lett.*, *30* (7), 1389, doi: 10.1029/2002GL016353, 2003.

Cunnold, D.M., E.-S. Yang, M.J. Newchurch, G.C.

Reinsel, J.M. Zawodny, and J.M. Russell III, Comment on "Enhanced upper stratospheric ozone: Sign of recovery or solar cycle effect?" by W. Steinbrecht et al., *J. Geophys. Res.*, *109*, D14305, doi: 10.1029/2004JD004826, 2004.

Dameris, M., V. Grewe, M. Ponater, R. Deckert, V. Eyring, F. Mager, S. Matthes, C. Schnadt, A. Stenke, B. Steil, C. Brühl, and M.A. Giorgetta, Long-term changes and variability in a transient simulation with a chemistry-climate model employing realistic forcing, *Atmos. Chem. Phys.*, *5*, 2121-2145, 2005.

Dameris, M., S. Matthes, R. Deckert, V. Grewe, and M. Ponater, Solar cycle effect delays onset of ozone recovery, *Geophys. Res. Lett.*, *33*, L03806, doi: 10.1029/2005GL024741, 2006.

de Grandpré, J., S.R. Beagley, V.I. Fomichev, E. Griffioen, J.C. McConnell, A.S. Medvedev, and T.G. Shepherd, Ozone climatology using interactive chemistry: Results from the Canadian Middle Atmosphere Model, *J. Geophys. Res.*, *105* (D21), 26475-26491, 2000.

Dhomse, S., M. Weber, I. Wohltmann, M. Rex, and J.P. Burrows, On the possible causes of recent increases in northern hemispheric total ozone from a statistical analysis of satellite data from 1979 to 2003, *Atmos. Phys. Chem.*, *6*, 1165-1180, 2006.

Douglass, A.R., M.R. Schoeberl, R.S. Stolarski, J.W. Waters, J.M. Russell III, A.E. Roche, and S.T. Massie, Interhemispheric differences in springtime production of HCl and $ClONO_2$ in the polar vortices, *J. Geophys. Res.*, *100* (D7), 13967-13978, 1995.

Douglass, A.R., R.S. Stolarski, S.E. Strahan, and B.C. Polansky, Sensitivity of Arctic ozone loss to polar stratospheric cloud volume and chlorine and bromine loading in a chemistry and transport model, *Geophys. Res. Lett., 33* (L17809), doi: 10.1029/2006GL026492, 2006.

Dvortsov, V.L., and S. Solomon, Response of the stratospheric temperatures and ozone to past and future increases in stratospheric humidity, *J. Geophys. Res.*, *106* (D7), 7505-7514, 2001.

Egorova, T., E. Rozanov, V. Zubov, E. Manzini, W. Schmutz, and T. Peter, Chemistry-climate model SOCOL: a validation of the present-day climatology, *Atmos. Chem. Phys.*, *5*, 1557-1576, 2005.

Eyring, V., N.R.P. Harris, M. Rex, T.G. Shepherd, D.W. Fahey, G.T. Amanatidis, J. Austin, M.P. Chipperfield, M. Dameris, P.M. de F. Forster, A. Gettelman, H.F. Graf, T. Nagashima, P.A. Newman, S. Pawson, M.J. Prather, J.A. Pyle, R.J. Salawitch, B.D. Santer, and D.W. Waugh, A strategy for process-oriented validation of coupled chemistry-climate models, *Bull. Amer. Meteorol. Soc.*, *86* (8), 1117-1133, 2005.

Eyring, V., N. Butchart, D.W. Waugh, H. Akiyoshi, J. Austin, S. Bekki, G.E. Bodeker, B.A. Boville, C. Brühl, M.P. Chipperfield, E. Cordero, M. Dameris, M. Deushi, V.E. Fioletov, S.M. Frith, R.R. Garcia, A. Gettelman, M.A. Giorgetta, V. Grewe, L. Jourdain, D.E. Kinnison, E. Mancini, E. Manzini, M. Marchand, D.R. Marsh, T. Nagashima, P.A. Newman, J.E. Nielsen, S. Pawson, G. Pitari, D.A. Plummer, E. Rozanov, M. Schraner, T.G. Shepherd, K. Shibata, R.S. Stolarski, H. Struthers, W. Tian, and M. Yoshiki, Assessment of temperature, trace species, and ozone in chemistry-climate model simulations of the recent past, *J. Geophys. Res., 111* (D22308), doi: 10.1029/2006JD007327, 2006.

Fleming, E.L., C.H. Jackman, R.S. Stolarski, and D.B. Considine, Simulation of stratospheric tracers using an improved empirically based two-dimensional model transport formulation, *J. Geophys. Res.*, *104* (D19), 23911-23934, 1999.

Giorgetta, M.A., and L. Bengtsson, The potential role of the quasi-biennial oscillation in the stratosphere-troposphere exchange as found in water vapor in general circulation model experiments, *J. Geophys. Res.*, *104* (D6), 6003-6019, 1999.

Grooß, J.-U., C. Brühl, and T. Peter, Impact of aircraft emissions on tropospheric and stratospheric ozone. Part I: Chemistry and 2-D model results, *Atmos. Environ.*, *32* (18), 3173-3184, 1998.

Hadjinicolaou, P., J.A. Pyle, and N.R.P. Harris, The recent turnaround in stratospheric ozone over northern middle latitudes: A dynamical modeling perspective, *Geophys. Res. Lett.*, *32*, L12821, doi: 10.1029/2005GL022476, 2005.

Hall, T.M., D.W. Waugh, K.A. Boering, and R.A. Plumb, Evaluation of transport in stratospheric models, *J. Geophys. Res.*, *104* (D15), 18815-18840, 1999.

Harris, J.M., S.J. Oltmans, P.P. Tans, R.D. Evans, and D.L. Quincy, A new method for describing long-term changes in total ozone, *Geophys. Res. Lett.*, *28* (24), 4535-4538, 2001.

Hauglustaine, D.A., J. Lathière, S. Szopa, and G.A. Folberth, Future tropospheric ozone simulated with a climate-chemistry-biosphere model, *Geophys. Res. Lett.*, *32*, L24807, doi: 10.1029/2005GL024031, 2005.

Hofmann, D.J., S.J. Oltmans, J.M. Harris, B.J. Johnson, and J.A. Lathrop, Ten years of ozonesonde measurements at the south pole: Implications for recovery of springtime Antarctic ozone, *J. Geophys. Res.*, *102* (D7), 8931-8943, 1997.

Hood, L.L., and B.E. Soukharev, Interannual variations of total ozone at northern midlatitudes correlated with stratospheric EP flux and potential vorticity, *J. Atmos. Sci.*, *62* (10), 3724-3740, 2005.

Hoppel, K., R. Bevilacqua, T. Canty, R.J. Salawitch, and M.L. Santee, A measurement/model comparison of ozone photochemical loss in the Antarctic ozone hole using Polar Ozone and Aerosol Measurement observations and the Match technique, *J. Geophys. Res.*, *110*, D19304, doi: 10.1029/2004JD005651, 2005.

IPCC (Intergovernmental Panel on Climate Change), *Special Report on Emissions Scenarios: A Special Report of Working Group III of the Intergovernmental Panel on Climate Change*, 599 pp., Cambridge University Press, Cambridge, U.K., 2000.

IPCC/TEAP (Intergovernmental Panel on Climate Change/Technology and Economic Assessment Panel), *IPCC/TEAP Special Report on Safeguarding the Ozone Layer and the Global Climate System: Issues Related to Hydrofluorocarbons and Perfluorocarbons*. Prepared by Working Groups I and III of the Intergovernmental Panel on Climate Change, and the Technical and Economic Assessment Panel, Cambridge University Press, U.K. and New York, 2005.

Isaksen, I.S.A., B. Rognerud, F. Stordal, M.T. Coffey, and W.G. Mankin, Studies of Arctic stratospheric ozone in a 2-D model including some effects of zonal asymmetries, *Geophys. Res. Lett.*, *17*, 557-560, 1990.

Jiang, Y., Y.L. Yung, and R.W. Zurek, Decadal evolution of the Antarctic ozone hole, *J. Geophys. Res.*, *101*, 8985-8999, 1996.

Kammen, D.M., and T.E. Lipman, Assessing the future hydrogen economy, *Science*, *302* (5643), 226-229, 2003.

Kirk-Davidoff, D.B., E.J. Hintsa, J.G. Anderson, and D.W. Keith, The effect of climate change on ozone depletion through changes in stratospheric water vapour, *Nature*, *402* (6760), 399-401, 1999.

Knudsen, B.M., N.R.P. Harris, S.B. Andersen, B. Christiansen, N. Larsen, M. Rex, and B. Naujokat, Extrapolating future Arctic ozone losses, *Atmos. Chem. Phys.*, *4*, 1849-1856, 2004.

Krzyścin, J.W., Change in ozone depletion rates beginning in the mid 1990s: Trend analyses of the TOMS/SBUV merged total ozone data, 1978-2003, *Ann. Geophys.*, *24*, 493-502, 2006.

Krzyścin, J.W., J. Jaroslawski, and B. Rajewska-Wiech, Beginning of the ozone recovery over Europe? - Analysis of the total ozone data from the ground-based observations, 1964-2004, *Ann. Geophys.*, *23*, 1685-1695, 2005.

Kurokawa, J., H. Akiyoshi, T. Nagashima, H. Masunaga, T. Nakajima, M. Takahashi, and H. Nakane, Effects of atmospheric sphericity on stratospheric chemistry and dynamics over Antarctica, *J. Geophys. Res.*, *110*, D21305, doi: 10.1029/2005JD005798, 2005.

Langematz, U., and M. Kunze, An update on dynamical changes in the Arctic and Antarctic stratospheric polar vortices, *Clim. Dyn.*, *27* (6), 647-660, 2006.

Lean, J, G.J. Rottman, H.L. Kyle, T.N. Woods, J.R. Hickey, and L.C. Puga, Detection and parameterization of variations in solar mid and near ultraviolet radiation (200-400 nm), *J. Geophys. Res.*, *102* (D25), 29939-29956, 1997.

Lefèvre, F., G.P. Brasseur, I. Folkins, A.K. Smith, and P. Simon, Chemistry of the 1991-1992 stratospheric winter: Three dimensional model simulations, *J. Geophys. Res*., *99* (D4), 8183-8195, 1994.

Levine, J.G., P. Braesicke, N.R.P. Harris, N.H. Savage, and J.A. Pyle, Pathways and timescales for troposphere-to-stratosphere transport via the tropical tropopause layer and their relevance for very short lived substances, *J. Geophys. Res.*, in press, 2006.

Malanca, F.E., P.O. Canziani, and G.A. Argüello, Trends evolution of ozone between 1980 and 2000 at mid-latitudes over the Southern Hemisphere: Decadal differences in trends, *J. Geophys. Res.*, *110*, D05102, doi: 10.1029/2004JD004977, 2005.

Manzini, E., B. Steil, C. Brühl, M.A. Giorgetta, and K. Krüger, A new interactive chemistry-climate model: 2. Sensitivity of the middle atmosphere to ozone depletion and increase in greenhouse gases and implications for recent stratospheric cooling, *J. Geophys. Res.*, *108* (D14), 4429, doi: 10.1029/2002JD002977, 2003.

McCormack, J.P., and L.L. Hood, Apparent solar cycle variations of upper stratospheric ozone and temperature: Latitude and seasonal dependences, *J. Geophys. Res.*, *101* (D15), 20933-20944, 1996.

McCormack, J.P., L.L. Hood, R. Nagatani, A.J. Miller, W.G. Planet, and R.D. McPeters, Approximate separation of volcanic and 11-year signals in the SBUV-SBUV/2 total ozone record over the 1979-1995 period, *Geophys. Res. Lett.*, *24* (22), 2729-2732, doi: 10.1029/97GL02900, 1997.

McLinden, C.A., S.C. Olsen, M.J. Prather, and J.B. Liley, Understanding trends in stratospheric NO_y and NO_2, *J. Geophys. Res.*, *106* (D21), 27787-27793, 2001.

Miller, A.J., A. Cai, G.C. Tiao, D.J. Wuebbles, L.E Flynn, S.-K. Yang, E.C. Weatherhead, V. Fioletov, I. Petropavlovskikh, X.-L. Meng, S. Guillas, R.M. Nagatani, and G.C. Reinsel, Examination of ozonesonde data for trends and trend changes incorporating solar and Arctic oscillation signals, *J. Geophys. Res.*, *111,* D13305, doi: 10.1029/2005JD006684, 2006.

Mote, P.W., K.H. Rosenlof, M.E. McIntyre, E.S. Carr, J.C. Gille, J.R. Holton, J.S. Kinnersley, H.C. Pumphrey, J.M. Russell, and J.W. Waters, An atmospheric tape recorder: the imprint of tropical tropopause temperatures on stratospheric water vapor, *J. Geophys. Res.*, *101* (D2), 3989-4006, 1996.

Nevison, C.D., S. Solomon, and R.S. Gao, Buffering interactions in the modeled response of stratospheric O_3 to increased NO_x and HO_x, *J. Geophys. Res.*, *104* (D3), 3741-3754, 1999.

Newchurch, M.J., E.-S. Yang, D.M. Cunnold, G.C. Reinsel, J.M. Zawodny, and J.M. Russell III, Evidence for slowdown in stratospheric ozone loss: First stage of ozone recovery, *J. Geophys. Res.*, *108* (D16), 4507, doi: 10.1029/2003JD003471, 2003.

Newman, P.A., S.R. Kawa, and E.R. Nash, On the size of the Antarctic ozone hole, *Geophys. Res. Lett.*, *31*, L21104, doi: 10.1029/2004GL020596, 2004.

Newman, P.A., E.R. Nash, S.R. Kawa, S.A. Montzka, and S.M. Schauffler, When will the Antarctic ozone hole recover?, *Geophys. Res. Lett.*, *33*, L12814, 2006.

Park, J.H., M.K.W. Ko, C.H. Jackman, R.A. Plumb, J.A. Kaye, and K.H. Sage, *Models and Measurements Intercomparison II*, *NASA/TM-1999-209554*, 502 pp., NASA Langley Research Center, Hampton, Va., 1999.

Park, M., W.J. Randel, D.E. Kinnison, R.R. Garcia, and W. Choi, Seasonal variation of methane, water vapor, and nitrogen oxides near the tropopause: Satellite observations and model simulations, *J. Geophys. Res.*, *109*, D03302, doi: 10.1029/2003JD003706, 2004.

Petropavlovskikh, I., C. Ahn, P.K. Bhartia, and L.E. Flynn, Comparison and covalidation of ozone anomalies and variability observed in SBUV(/2) and Umkehr northern midlatitude ozone profile estimates, *Geophys. Res. Lett.*, *32*, L06805, doi: 10.1029/2004GL022002, 2005.

Pitari, G., Interactive comment on "Extrapolating future Arctic ozone losses" by B.M. Knudsen et al., *Atmos. Chem. Phys. Discuss.*, *4*, S1214-S1215, 2004.

Pitari, G., E. Mancini, V. Rizi, and D.T. Shindell, Impact of future climate change and emission changes on stratospheric aerosols and ozone, *J. Atmos. Sci.*, *59* (3), 414-440, 2002.

Portmann, R.W., S.S. Brown, T. Gierczak, R.K. Talukdar, J.B. Burkholder, and A.R. Ravishankara, Role of nitrogen oxides in the stratosphere: A reevaluation based on laboratory studies, *Geophys. Res. Lett.*, *26* (15), 2387-2390, 1999.

Prather, M., and D. Ehhalt (Co-ordinating Lead Authors), F. Dentener, R. Derwent, E. Dlugokencky, E. Holland, I. Isaksen, J. Katima, V. Kirchhoff, P. Matson, P. Midgley, and M. Wang, Atmospheric chemistry and greenhouse gases, Chapter 4 in *Climate Change 2001: The Scientific Basis: Contribution of Working Group I to the Third Assessment Report of the Intergovernmental Panel on Climate Change*, edited by J.T. Houghton, Y. Ding, D.J. Griggs, M. Noguer, P.J. van der Linden, X. Dai, K. Maskell, and C.A. Johnson, 881 pp., Cambridge University Press, Cambridge, U.K., 2001.

Pyle, J.A., P. Braesicke, and G. Zeng, Dynamical variability in the modelling of chemistry-climate interactions, *Faraday Discuss.*, *130*, 27-39, doi: 10.1039/b417947c, 2005.

Randeniya, L.K., P.F. Vohralik, and I.C. Plumb, Stratospheric ozone depletion at northern mid latitudes in the 21st century: The importance of future concentrations of greenhouse gases nitrous oxide and methane, *Geophys. Res. Lett.*, *29* (4), 1051, doi: 10.1029/2001GL014295, 2002.

Rayner, N.A., D.E. Parker, E.B. Horton, C.K. Folland, L.V. Alexander, D.P. Rowell, E.C. Kent, and A. Kaplan, Global analyses of sea surface temperature, sea ice, and night marine air temperature since the late nineteenth century, *J. Geophys. Res.*, *108* (D14), 4407, doi: 10.1029/2002JD002670, 2003.

Reinsel, G.C., Trend analysis of upper stratospheric Umkehr ozone data for evidence of turnaround, *Geophys. Res. Lett.*, *29* (10), 1451, doi: 10.1029/2002GL014716, 2002.

Reinsel, G.C., E. Weatherhead, G.C. Tiao, A.J. Miller, R.M. Nagatani, D.J. Wuebbles, and L.E. Flynn, On detection of turnaround and recovery in trend for ozone, *J. Geophys. Res.*, *107* (D10), 4078, doi: 10.1029/2001JD000500, 2002.

Reinsel, G.C., A.J. Miller, E.C. Weatherhead, L.E. Flynn, R.M. Nagatani, G.C. Tiao, and D.J. Wuebbles, Trend analysis of total ozone data for turnaround and dynamical contributions, *J. Geophys. Res.*, *110*, D16306, doi: 10.1029/2004JD004662, 2005.

Rex, M., R.J. Salawitch, P. von der Gathen, N.R.P. Harris, M.P. Chipperfield, and B. Naujokat, Arctic ozone loss and climate change, *Geophys. Res. Lett.*, *31*,

L04116, doi: 10.1029/2003GL018844, 2004.

Richter, J.H., and R.R. Garcia, On the forcing of the mesospheric semi-annual oscillation in the Whole Atmosphere Community Climate Model, *Geophys. Res. Lett.*, *33*, L01806, doi: 10.1029/2005GL024378, 2006.

Rinsland, C.P., D.K. Weisenstein, M.K.W. Ko, C.J. Scott, L.S. Chiou, E. Mahieu, R. Zander, and P. Demoulin, Post-Mount Pinatubo eruption ground-based infrared stratospheric column measurements of HNO_3, NO, and NO_2 and their comparison with model calculations, *J. Geophys. Res.*, *108* (D15), 4437, doi: 10.1029/2002JD002965, 2003.

Rosenfield, J.E., and M.R. Schoeberl, Recovery of the tropical lower stratospheric ozone layer, *Geophys. Res. Lett.*, *32*, L21806, doi: 10.1029/2005GL023626, 2005.

Rosenfield, J.E., D.B. Considine, P.E. Meade, J.T. Bacmeister, C.H. Jackman, and M.R. Schoeberl, Stratospheric effects of Mount Pinatubo aerosol studied with a coupled two-dimensional model, *J. Geophys. Res.*, *102* (D3), 3649-3670, 1997.

Rosenfield, J.E., A.R. Douglass, and D.B. Considine, The impact of increasing carbon dioxide on ozone recovery, *J. Geophys. Res.*, *107* (D6), 4049, doi: 10.1029/2001JD000824, 2002.

Rozanov, E., M. Schraner, C. Schnadt, T. Egorova, M. Wild, A. Ohmura, V. Zubov, W. Schmutz, and Th. Peter, Assessment of the ozone and temperature variability during 1979-1993 with the chemistry-climate model SOCOL, *Adv. Space Res.*, *35* (8), 1375-1384, 2005.

Ruzmaikin, A., J. Lawrence, and C. Cadavid, A simple model of stratospheric dynamics including solar variability, *J. Clim.*, *16* (10), 1593-1600, 2003.

Salawitch, R.J., D.K. Weisenstein, L.J. Kovalenko, C.E. Sioris, P.O. Wennberg, K. Chance, M.K.W. Ko, and C.A. McLinden, Sensitivity of ozone to bromine in the lower stratosphere, *Geophys. Res. Lett.*, *32*, L05811, doi: 10.1029/2004GL021504, 2005.

Salby, M.L., and P.F. Callaghan, Systematic changes of Northern Hemisphere ozone and their relationship to random interannual changes, *J. Clim.*, *17* (23), 4512-4521, 2004.

Santee, M.L., G.L. Manney, W.G. Read, L. Froidevaux, and J.W. Waters, Polar vortex conditions during the 1995-96 Arctic winter: MLS ClO and HNO_3, *Geophys. Res. Lett.*, *23* (22), 3207-3210, 1996.

Shibata, K., and M. Deushi, Radiative effect of ozone on the quasi-biennial oscillation in the equatorial stratosphere, *Geophys. Res. Lett.*, *32*, L24802, doi: 10.1029/2005GL023433, 2005.

Shibata, K., M. Deushi, T.T. Sekiyama, and H. Yoshimura, Development of an MRI chemical transport model for the study of stratospheric chemistry, *Pap. Meteorol. Geophys.*, *55* (3/4), 75-119, 2005.

Smyshlyaev, S.P., V.L. Dvortsov, M.A. Geller, and V.A. Yudin, A two-dimensional model with input parameters from a general circulation model: Ozone sensitivity to different formulations for the longitudinal temperature variation, *J. Geophys. Res.*, *103* (D21), 28373-28387, 1998.

Solomon, S., R.W. Portmann, R.R. Garcia, L.W. Thomason, L.R. Poole, and M.P. McCormick, The role of aerosol variations in anthropogenic ozone depletion at northern midlatitudes, *J. Geophys. Res.*, *101*, 6713-6728, doi: 10.1029/95JD03353, 1996.

Solomon, S., R.W. Portmann, T. Sasaki, D.J. Hofmann, and D.W.J. Thompson, Four decades of ozonesonde measurements over Antarctica, *J. Geophys. Res.*, *110*, D21311, doi: 10.1029/2005JD005917, 2005.

Steil, B., C. Brühl, E. Manzini, P.J. Crutzen, J. Lelieveld, P.J. Rasch, E. Roeckner, and K. Krüger, A new interactive chemistry climate model: 1. Present-day climatology and interannual variability of the middle atmosphere using the model and 9 years of HALOE/UARS data, *J. Geophys. Res.*, *108* (D9), 4290, doi: 10.1029/2002JD002971, 2003.

Steinbrecht, W., H. Claude, and P. Winkler, Enhanced upper stratospheric ozone: Sign of recovery or solar cycle effect?, *J. Geophys. Res.*, *109*, D02308, doi: 10.1029/2003JD004284, 2004a.

Steinbrecht, W., H. Claude, and P. Winkler, Reply to comment by D. M. Cunnold et al. on "Enhanced upper stratospheric ozone: Sign of recovery or solar cycle effect?", *J. Geophys. Res.*, *109*, D14306, doi: 10.1029/2004JD004948, 2004b.

Steinbrecht, W., H. Claude, F. Schönenborn, I.S. McDermid, T. Leblanc, S. Godin, T. Song, D.P.J. Swart, Y.J. Meijer, G.E. Bodeker, B.J. Connor, N. Kämpfer, K. Hocke, Y. Calisesi, N. Schneider, J. de la Nöe, A.D. Parrish, I.S. Boyd, C. Brühl, B. Steil, M.A. Giorgetta, E. Manzini, L.W. Thomason, J.M. Zawodny, M.P. McCormick, J.M. Russell, P.K. Bhartia, R.S. Stolarski, and S.M. Hollandsworth-Frith, Long-term evolution of upper stratospheric ozone at selected stations of the Network for the Detection of Stratospheric Change (NDSC), *J. Geophys. Res.*, *111*, D10308, doi: 10.1029/2005JD006454, 2006a.

Steinbrecht, W., B. Haßler, C. Brühl, M. Dameris, M.A. Giorgetta, V. Grewe, E. Manzini, S. Matthes, C. Schnadt, B. Steil, and P. Winkler, Interannual vari-

ation patterns of total ozone and lower stratospheric temperature in observations and model simulations, *Atmos. Chem. Phys.*, *6*, 349-374, 2006b.

Stolarski, R.S., A.R. Douglass, S. Steenrod, and S. Pawson, Trends in stratospheric ozone: Lessons learned from a 3D chemical transport model, *J. Atmos. Sci.*, *63* (3), 1028-1041, 2006.

Stordal, F., I.S.A. Isaksen, and K. Horntveth, A diabatic circulation two-dimensional model with photochemistry: Simulations of ozone and long-lived tracers with surface sources, *J. Geophys. Res.*, *90*, 5757-5776, 1985.

Struthers, H., K. Kreher, J. Austin, R. Schofield, G.E. Bodeker, P.V. Johnston, H. Shiona, and A. Thomas, Past and future simulations of NO_2 from a coupled chemistry-climate model in comparison with observations, *Atmos. Chem. Phys.*, *4*, 2227-2239, 2004.

Tarasick, D.W., V.E. Fioletov, D.I. Wardle, J.B. Kerr, and J. Davies, Changes in the vertical distribution of ozone over Canada from ozonesondes: 1980-2001, *J. Geophys. Res.*, *110*, D02304, doi: 10.1029/2004 JD004643, 2005.

Tian, W., and M.P. Chipperfield, A new coupled chemistry-climate model for the stratosphere: The importance of coupling for future O_3-climate predictions, *Quart. J. Roy. Meteorol. Soc.*, *131* (605), 281-303, 2005.

Tiao, G.C., D. Xu, J.H. Pedrick, X. Zhu, and G.C. Reinsel, Effects of autocorrelation and temporal sampling schemes on estimates of trend and spatial correlation, *J. Geophys. Res.*, *95*, 20507-20517, 1990.

Tie, X.X., and G. Brasseur, The response of stratospheric ozone to volcanic eruptions: Sensitivity to atmospheric chlorine loading, *Geophys. Res. Lett.*, *22* (22), 3035-3038, 1995.

Tromp, T.K., R.-L. Shia, M. Allen, J.M. Eiler, and Y.L. Yung, Potential environmental impact of a hydrogen economy on the stratosphere, *Science*, *300* (5626), 1740-1742, 2003.

Velders, G.J.M., *Scenario Study of the Effects of CFC*, *HCFC*, *and HFC Emissions on Stratospheric Ozone*, *RIVM Report 722201006*, 99 pp., National Institute of Public Health and the Environment, Bilthoven, The Netherlands, 1995.

Warwick, N.J., S. Bekki, E.G. Nisbet, and J.A. Pyle, Impact of a hydrogen economy on the stratosphere and troposphere studied in a 2-D model, *Geophys. Res. Lett.*, *31*, L05107, doi: 10.1029/2003 GL019224, 2004.

Weatherhead, E.C., and S.B. Andersen, The search for signs of recovery of the ozone layer, *Nature*, *441* (7089), 39-45, doi: 10.1038/nature04746, 2006.

Weatherhead, E.C., G.C. Reinsel, G.C. Tiao, C.H. Jackman, L. Bishop, S.M. Hollandsworth Frith, J. DeLuisi, T. Keller, S.J. Oltmans, E.L. Fleming, D.J. Wuebbles, J.B. Kerr, A.J. Miller, J. Herman, R.D. McPeters, R.M. Nagatani, and J.E. Frederick, Detecting the recovery of total column ozone, *J. Geophys. Res.*, *105* (D17), 22201-22210, 2000.

WMO (World Meteorological Organization), *Scientific Assessment of Ozone Depletion: 2002*, *Global Ozone Research and Monitoring Project–Report No. 47*, Geneva, Switzerland, 2003.

Yang, E.-S., D.M. Cunnold, M.J. Newchurch, and R.J. Salawitch, Change in ozone trends at southern high latitudes, *Geophys. Res. Lett.*, *32*, L12812, doi: 10.1029/2004GL022296, 2005.

Yang, E.-S., D.M. Cunnold, R.J. Salawitch, M.P. McCormick, J. Russell III, J.M. Zawodny, S. Oltmans, and M.J. Newchurch, Attribution of recovery in lower-stratospheric ozone, *J. Geophys. Res.*, *111* (D17309), doi: 10.1029/2005JD006371, 2006.

Appendix 6A
Model Scenarios

Table 6A-1 lists the forcings used in the 2-D model and Chemistry-Climate Model (CCM) simulations. Two reference and two sensitivity simulations along with a set of model forcings have been proposed as part of the CCM Validation Activity for the Stratospheric Processes and their Role in Climate (SPARC) project of the World Climate Research Programme (Eyring et al., 2005) to assess the near-term and long-term evolution of stratospheric ozone. Unless otherwise stated, both types of models used changes in halocarbons as prescribed in Table 4B-2 of WMO (2003), WMGHGs based on the IPCC (2000) Special Report on Emissions Scenarios (SRES) A1B scenario, and sulfate aerosols for 1979 to 1999 based on the climatology of David Considine (NASA Langley Research Center; see http://www.pa.op.dlr.de/CCMVa/Forcings/CCMVal_Forcings.html) with background values thereafter.

The sea surface temperatures (SSTs) in the CCMs are prescribed from observations (HadSST1) in past simulations (Rayner et al., 2003). For REF2/SCN2 simulations they come either from the underlying IPCC coupled-ocean model simulation or from the UK Meteorological Office HadGEM1 simulations using IPCC SRES scenario A1B. In the reference past simulations (REF1), the quasi-biennial oscillation (QBO) is either prescribed (Giorgetta and Bengtsson, 1999) or internally generated, and the influence of the 11-year solar cycle on photolysis rates is parameterized according to the intensity of the 10.7 cm radiation of the Sun (Lean et al., 1997). In future runs, the solar cycle and an external QBO forcing are only considered in SCN2, but not in REF2.

In the CCMVal halogen file (i) The data from Table 4B-2 of WMO (2003), which were given every 5 years, were linearly interpolated into monthly values; (ii) The data for each year in Table 4B-2 were interpreted as the midpoint of each year rather than the correct 1st of the year; and (iii) Halon-2402 was mistakenly not included. Assumptions (i) and (ii) result in a slightly smaller peak organic chlorine (CCl_y) than observed (3.56 ppb instead of 3.58 ppb) and the peak occurs 2.4 years too late, while assumption (iii) results in organic bromine (CBr_y) that is around 1 ppt too low at the peak. To test the sensitivity of these assumptions on ozone, one 2-D model has been used to rerun the simulation with a corrected Ab halogen scenario. The difference between the two simulations is very small (especially compared with the differences between models), and none of the conclusions from the analysis of the 2-D models or CCMs are affected by the differences in the halogen forcing.

Table 6A-1. Model simulations.

Run [1]	Period	Motivation	Halocarbons	WMGHGs	SSTs [2]	Solar Variability	QBO
P1	1979-2004	Past Trends	WMO (2003) Table 4B-2	IPCC (2000) A1B	N/A	None	None
F1	2005-2100	Future, Control	WMO (2003) Table 4B-2	IPCC (2000) B1	N/A	None	None
REF1	1960/1980-2004	Past Trends	WMO (2003) Table 4B-2	IPCC (2000) A1B	Observed (HadISST1)	Observed (MAVER)	Forced or internally generated
REF2	1960/1980-2100	Future, Control	WMO (2003) Table 4B-2	IPCC (2000) A1B	Modeled	None	Only internally generated
SCN2	1980-2025	Solar Cycle and QBO	WMO (2003) Table 4B-2	IPCC (2000) A1B	Modeled	Observed + repeating in future	Forced or internally generated
NCC	1970-2050	Fixed GHGs	WMO (2003) Table 4B-2	Fixed at start of simulation	Observed 1970-79 repeating or modeled	As in REF1/REF2/SCN2	Forced or internally generated

[1] P1 and F1 runs are for 2-D models, and remainder are for CCMs.

[2] Applies to CCM simulations only.